Catalysis Today 185 (2012) 2–16

Contents lists available at SciVerse ScienceDirect

Catalysis Today

journal homepage: www.elsevier.com/locate/cattod

Modified Pd catalysts for the selective hydrogenation of acetylene

Woo-Jae Kim [a], Sang Heup Moon [b,*]

[a] Division of Energy and Biological Engineering, Kyungwon University, Seongnam, Gyeonggi-do 461-701, Republic of Korea
[b] School of Chemical and Biological Engineering, Seoul National University, Seoul 151-744, Republic of Korea

ARTICLE INFO

Article history:
Received 23 June 2011
Received in revised form
21 September 2011
Accepted 27 September 2011
Available online 22 October 2011

Keywords:
Acetylene hydrogenation
Si
SMSI
Cu
Selective deposition
Structure sensitivity

ABSTRACT

This article reviews our previous studies to develop high performance catalysts for acetylene hydrogenation. Ethylene selectivity of Pd catalysts in acetylene hydrogenation was improved by adding Si, metal oxides showing SMSI behavior, and either Ag or Cu as promoters. The promoter effect was further enhanced by maximizing the interactions between Pd and added promoters. Chemical vapor deposition was used for the addition of Si, high-temperature reduction for the SMSI metal oxides, and a surface redox (SR) for Ag and Cu. Si modified the Pd surface geometrically, SMSI metal oxides modified Pd both electronically and geometrically, and Ag modified Pd largely electronically. Cu added by SR modified Pd electronically to a small extent, but preferentially decorated the low-coordination sites of Pd such that the ethylene selectivity of the optimum catalyst was significantly promoted from that of Pd, while its activity remained comparable to that of Pd. The sensitivity of ethylene selectivity to the surface structure of Pd was demonstrated using model catalysts containing uniform-sized Pd particles in either cubic or spherical shapes. The three stage deactivation of the Pd catalyst and the self-regenerative behavior in early stages of deactivation were also investigated.

1. Introduction

An ethylene stream from a naphtha cracker unit typically contains about 0.1–1% of acetylene as an impurity, which is required to be removed to less than 5 ppm because it poisons the catalyst in ensuing ethylene polymerization processes and eventually degrades the quality of the produced polyethylene [1,2]. Acetylene impurities are usually removed by two methods, that is, adsorption with zeolite [3] and conversion to ethylene by selective hydrogenation using Pd catalysts [2], the latter more commonly being used.

Two factors are the keys to the assessment of this process. One is the ethylene selectivity [4], i.e., the fraction of ethylene produced by acetylene conversion, and the other is the catalyst lifetime which is limited by green oil deposition during the reaction [5].

Various additives, such as Ag, Ni, Cu, Pb, Tl, Cr, and K, have been reported to improve the performance of Pd catalysts, especially in achieving a high selectivity for ethylene production [6–12]. The role of additives, or selectivity promoters, is generally considered to be derived from two factors: geometric [8,13] and electronic [6,11]. For example, Leviness et al. [8] reported the promotion of ethylene selectivity upon Cu addition, which they proposed to be due to a geometric effect. That is, the insertion of Cu into the Pd matrix decreases the number of multi-coordination sites of the Pd responsible for the dissociative adsorption of acetylene and suppresses the formation of beta phase Pd hydride as well; both are damaging to ethylene selectivity. On the other hand, Huang et al. [6] reported an improved selectivity on Ag-promoted Pd catalysts, suggesting that an increase in the Pd d-band electron density upon Ag addition was responsible for the selectivity enhancement.

To design a novel catalyst with improved performance in acetylene hydrogenation, it is necessary to consider the reaction mechanism for acetylene hydrogenation, which consists of several reaction paths, as shown in Fig. 1 [14]. Path I is the partial hydrogenation pathway of acetylene to ethylene, which is either desorbed as the major gaseous ethylene product (Path II) or further hydrogenated to ethane (Path III). Consequently, ethylene selectivity can be improved by promoting Path II and suppressing Path III, for which two methods are typically used in industrial processes. One is to add a moderator chemical to the reaction stream, e.g., CO, which adsorbs more strongly on Pd than ethylene and, consequently, facilitates ethylene desorption from the catalyst surface (Path II) [15]. The other is to maintain a low H_2/acetylene ratio in the feed such that the catalyst surface is deficient in hydrogen concentration, thus the full hydrogenation of ethylene (Path III) is retarded [16,17]. Path IV, allowing the direct full hydrogenation of acetylene to ethane, is insignificant at high acetylene coverage and low partial pressures of hydrogen [18], which is the case in most industrial processes. The triply adsorbed species, ethylidyne, had been suggested as an intermediate in Path IV [8,18–20] but was

* Corresponding author. Tel.: +82 2 880 7409; fax: +82 2 875 6697.
E-mail address: shmoon@surf.snu.ac.kr (S.H. Moon).

0920-5861/$ – see front matter © 2011 Elsevier B.V. All rights reserved.
doi:10.1016/j.cattod.2011.09.037

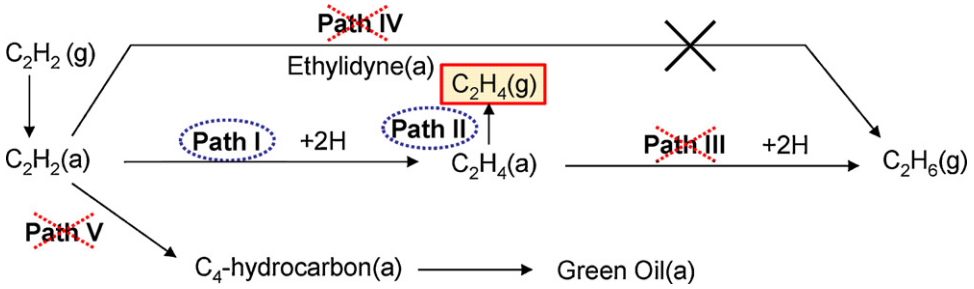

Fig. 1. Reaction paths of acetylene hydrogenation [14].

later verified to be a simple spectator of surface reactions [21,22]. Path V, which allows for the dimerization of the C_2 species, eventually leads to catalyst deactivation via the accumulation of green oil [23,24]. Path V also lowers the ethylene selectivity because it consumes acetylene without producing ethylene. Accordingly, the mechanism of acetylene hydrogenation indicates that, for improving ethylene selectivity and suppressing green oil formation, Paths I and II should be promoted while the other paths should be suppressed.

Our research efforts for the development of a high performance acetylene hydrogenation catalyst, both in ethylene selectivity and catalyst lifetime, focused on selectively manipulating the electronic and geometric structure of the Pd catalyst by incorporating new promoters [13,14,25–30], selectively depositing promoters on specific Pd surfaces [13,14,25–32], and controlling the shape of the Pd particles [33]: (1) Si was selectively deposited on Pd active sites over SiO_2 or Al_2O_3 support using a chemical vapor deposition (CVD) method as a geometric modifier, such that the number of multi-coordination sites of the Pd surface was effectively suppressed leading to the high ethylene selectivity [13,25] and a decrease in green oil formation [27]; (2) metal oxides exhibiting phenomenon similar to strong metal–support interaction (SMSI) were added to the Pd catalyst as a geometric and electronic modifier, such that the adsorption strength of reagents as well as multi-coordination sites of Pd surface were effectively controlled, leading to the high ethylene selectivity [14,26,30] and suppression of green oil formation [29]; (3) Pd sites were decorated with a promoter added by surface reduction method (SR), such that specific Pd structure responsible for lowering ethylene selectivity was effectively blocked [31,32].

This article reviews our previous studies based on the above three strategies.

2. Si-modified Pd catalysts prepared by selective CVD

2.1. Selective deposition of Si on the Pd surface

The Pd surface in Pd/SiO_2 was modified with Si deposited on the Pd surface by silane (SiH_4) decomposition and its catalytic performance in acetylene hydrogenation was investigated. Pd/SiO_2, used as a model catalyst, was prepared by an ion exchange method using $Pd(NH_3)_4(OH)_2$, and the Si-modified catalyst, $Pd–Si/SiO_2$, was prepared by selectively depositing Si on the Pd surface as previously reported [13]. 1% SiH_4/H_2 mixture was injected as pulses into the H_2 stream flowing through a reactor that contained the pre-reduced Pd catalyst and was maintained at 250 °C. The amount of deposited Si was controlled by the number of repetitive injections. After the Si deposition, the reactor was cooled to room temperature and the catalyst was exposed to O_2 for 1 h such that the Si species deposited on the Pd surface was oxidized.

2.2. Catalytic performance of Si-modified catalyst

The catalytic performance of the Si-modified Pd catalyst ($Pd–Si/SiO_2$) in acetylene hydrogenation was compared with that of an un-modified one (Pd/SiO_2) with respect to two key factors: ethylene selectivity and catalyst deactivation.

Fig. 2 shows typical results of acetylene hydrogenation obtained on Pd/SiO_2 and $Pd–Si/SiO_2$ over a wide conversion range [13]. Obviously, the ethylene selectivity increased when the catalyst was modified with Si, while acetylene conversion was slightly lowered upon Si addition. The added Si appears to be a promoter for ethylene selectivity rather than for the hydrogenation activity of the Pd catalyst.

The extent of catalyst deactivation by green oil formation was also analyzed for both catalysts [27]. Pd/SiO_2 and $Pd–Si/SiO_2$ were deactivated, with the same level of acetylene conversion and the reaction rates of both catalysts were plotted as normalized values to their initial reaction rates against the accumulated amounts of acetylene conversion in Fig. 3. Obviously, the catalyst deactivation was suppressed on $Pd–Si/SiO_2$ (b-1) compared to that on Pd/SiO_2 (a-1). Pd catalysts used in acetylene hydrogenation are deactivated largely due to the accumulation of green oil on the Pd active sites [34]. The above findings suggest that Si addition has a beneficial effect on the catalytic performance of the Pd catalyst in acetylene hydrogenation by increasing ethylene selectivity as well as decreasing green oil formation.

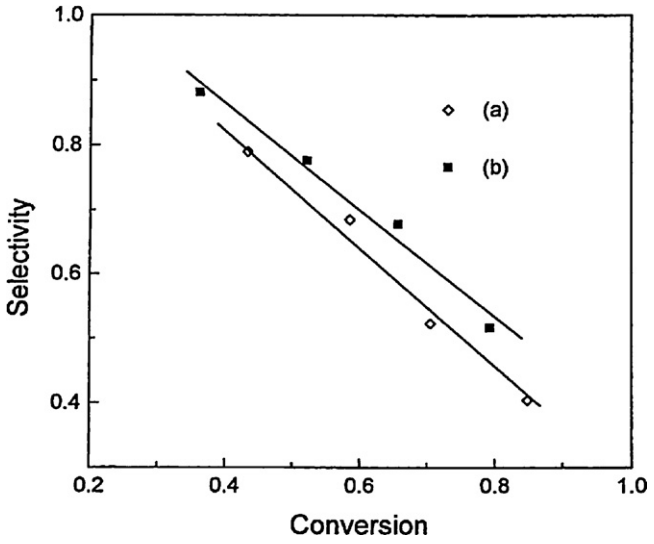

Fig. 2. Ethylene selectivity versus conversion in acetylene hydrogenation (H_2/acetylene = 2, T = 60 °C): (a) Pd/SiO_2; (b) $Pd–Si/SiO_2$ (Si/Pd = 0.095) [13].

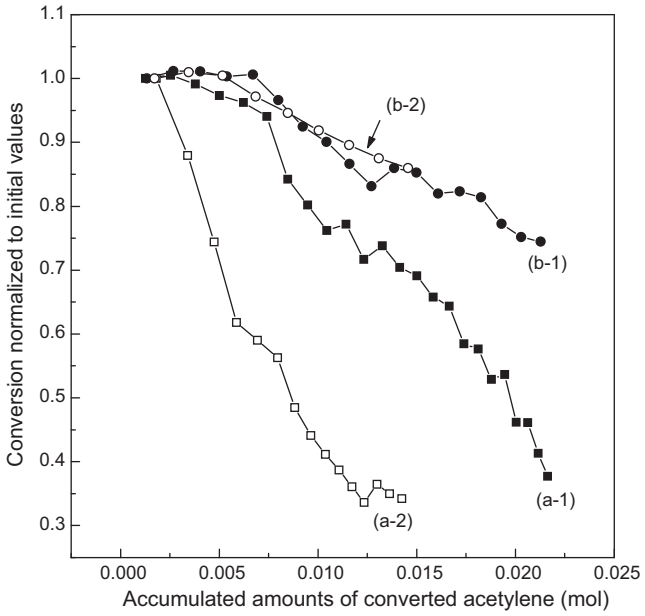

Fig. 3. Deactivation of catalyst, before and after regeneration, with accumulated amounts of converted acetylene (regeneration condition: O_2 = 20 ml/min, temperature = 600 °C for 2 h): (a) Pd/SiO_2; (b) $Pd–Si/SiO_2$: (1) fresh; (2) after regeneration [27].

2.3. The role of Si in selectivity enhancement

To further investigate the surface modification of Pd by the added Si, we monitored changes in the geometric and electronic structure of the Pd catalyst upon Si addition. Fig. 4 compares IR spectra of CO adsorbed on Pd/SiO_2 and $Pd–Si/SiO_2$ [13]. The overall spectral intensity decreases with Si addition, because the number of Pd active sites for CO adsorption was reduced due to the coverage of Pd with added Si. The above trend was also confirmed by CO chemisorption results showing a decrease in the absolute amount of adsorbed CO on Pd due to Si addition [13]. A striking feature in Fig. 4 is that the spectral intensity of a sharp band at 1995 cm^{-1}, assigned to the compressed bridged CO bond, decreases rapidly with Si deposition. CO adsorbs on Pd in four modes [35]: linear, compressed-bridged, isolated-bridged, and tri-coordinated bonds. The compressed-bridged mode of CO adsorption requires three adjacent Pd atoms, while the

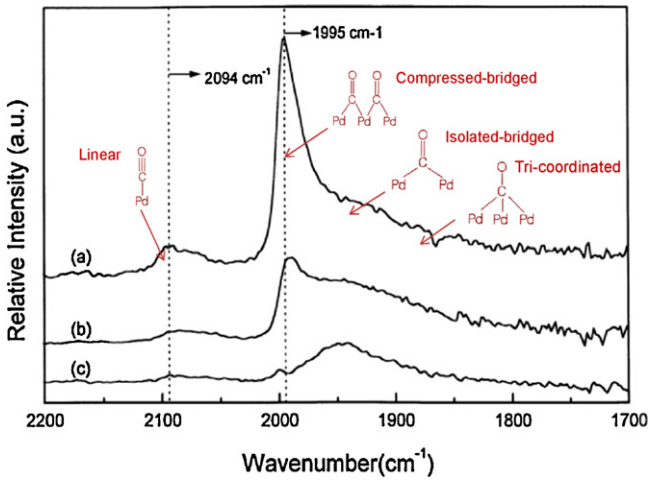

Fig. 4. IR spectra of CO adsorbed on various catalysts: (a) Pd/SiO_2; (b) $Pd–0.095Si/SiO_2$; (c) $Pd–0.19Si/SiO_2$ [13].

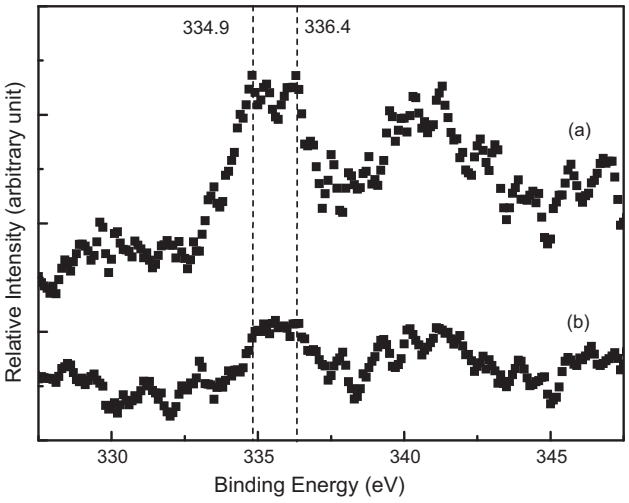

Fig. 5. XPS of Pd $3d_{5/2}$ on (a) Pd/SiO_2 and (b) $Pd–Si/SiO_2$ [25].

isolated-bridged mode requires only two. When Si is selectively deposited on the Pd surface, it is expected that the sites requiring three adjacent Pd atoms are blocked more rapidly over the sites requiring two atoms. Accordingly, the CO-IR results provide evidence that the multi-coordination sites of Pd are effectively inhibited by Si deposition.

To investigate if the added Si changes the electronic configuration of Pd, we performed XPS analysis on Pd/SiO_2 and $Pd–Si/SiO_2$. Fig. 5 shows that the binding energy of Pd $3_{5/2}$ electrons for both catalysts positioned in the range of 334.9–336.4 eV [25]. Upon Si addition, the overall peak intensity decreased, however, a peak shift was not observed, indicating that the added Si did not affect the electronic structure of Pd. Changes in the Pd electronic structure by alloy formation between Si and Pd during Si deposition on Pd have been reported in the literature [36,37]. However, this phenomenon was not observed in our system, possibly due to the oxidation of Si during catalyst preparation, turning Pd–Si alloy into Pd and segregated SiO_2 on the Pd surface.

We further investigated how the adsorption behavior of reactants and reaction intermediates was affected by the geometric modification of Pd by added Si. Fig. 6 shows the isotherms for hydrogen adsorbed on Pd/SiO_2 and $Pd–Si/SiO_2$. The isotherms were obtained in two steps for each catalyst as described in our previous study [25]. Two significant changes in the hydrogen adsorption behavior were observed upon Si addition. The amount of strongly chemisorbed hydrogen on the Pd surface, which was measured by the gap between the two isotherms, was significantly reduced and the amount of weakly adsorbed hydrogen, which was measured by the second isotherm, increased upon Si addition. Consequently, the catalyst surface was covered more with weakly adsorbed hydrogen than with strongly chemisorbed hydrogen upon Si addition. The suppression of hydrogen chemisorption on $Pd–Si/SiO_2$ was possibly due to the presence of Si species on the Pd surface, which reduced the multi-coordination sites of Pd leading to the suppression of the dissociative adsorption of hydrogen on the Pd surface. The weakening of the hydrogen adsorption strength on Pd due to an increase in the Pd–H bond distance, thus leading to a decrease in the bond strength by the added second metal species, has also been reported in many studies [36,38,39]. The suppression of hydrogen adsorption on Pd by Si addition is likely to suppress Path III in the mechanism of acetylene hydrogenation.

Fig. 7 shows TPD patterns of ethylene adsorbed on either Pd/SiO_2 or $Pd–Si/SiO_2$, obtained by monitoring the mass signal of m/e = 27 [25]. Pd/SiO_2 exhibited two major peaks, which might be assigned as follows [40]. The peak centered at 62 °C represents

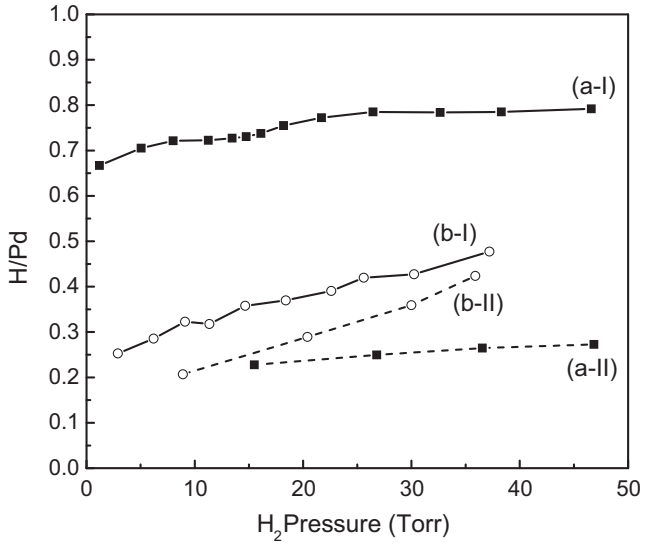

Fig. 6. Hydrogen isotherms: (a-I) first isotherm of Pd/SiO_2; (a-II) second isotherm of Pd/SiO_2; (b-I) first isotherm of $Pd–Si/SiO_2$; (b-II) second isotherm of $Pd–Si/SiO_2$ [25].

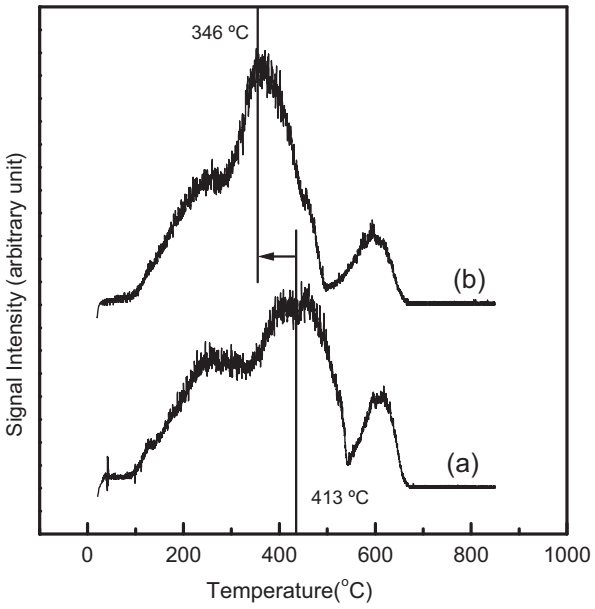

Fig. 8. Differential thermogravimetric analysis of used catalysts in air: (a) Pd/SiO_2; (b) $Pd–Si/SiO_2$ [27].

weakly adsorbed π-bonded ethylene, which consequently desorbs without decomposition. The peak centered at 105 °C represents di-σ-bonded ethylene, which undergoes decomposition followed by the recombination with hydrogen to produce ethylene as well as ethane. In the case of $Pd–Si/SiO_2$, the peak at 105 °C was significantly reduced. This result suggests that ethylene was desorbed more easily from the surface of $Pd–Si/SiO_2$ than from Pd/SiO_2, which supports the observed selectivity improvement on the Si-modified catalyst.

2.4. The role of added Si in the suppression of catalyst deactivation

Previous studies [41,42] have revealed that green oil is formed through the polymerization of C_2 hydrocarbons, which preferentially proceeds on multi-coordination sites of Pd. Considering that the added Si effectively dilutes the multi-coordination sites of Pd, as confirmed by CO-IR results (Fig. 4), the above results suggest that green oil formed on $Pd–Si/SiO_2$ may be short in chain length and its amount is small compared to that formed on Pd/SiO_2. Fig. 8 shows DTGA results of both catalysts, where three major peaks were observed in different temperature regions [27]: Peak I (below 300 °C) for heavy hydrocarbons adsorbed on the catalyst surface or absorbed in the catalyst pores, Peak II (300–500 °C) for coke on or in the vicinity of Pd, and Peak III (above 500 °C) for coke produced on the support without the influence of Pd [23]. A notable change in Fig. 8 is that the average position of Peak II is significantly shifted to lower temperatures, by 67 °C, due to the Si modification, indicating that the green oil formed on or in the vicinity of Pd became more volatile upon Si addition. This result is in accordance with green oil-IR results where the average carbon number of green oil is lowered from 26 to 19.4 upon Si addition [27]. Conclusively, the effective blocking of the multi-coordination adsorption sites of Pd by the Si species suppresses the formation of green oil on the surface (Path V in the mechanism of acetylene hydrogenation (Fig. 1)) and reduces catalyst deactivation rates during acetylene hydrogenation.

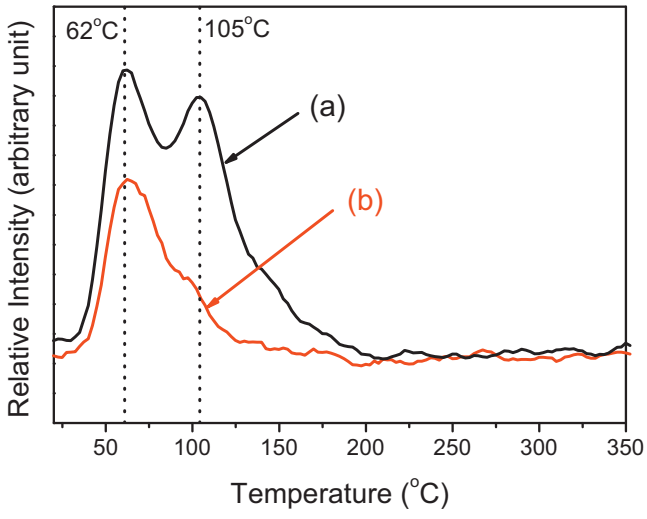

Fig. 7. Changes in the mass ($m/e = 27$) signal during temperature-programmed desorption of ethylene from (a) Pd/SiO_2 and (b) $Pd–Si/SiO_2$ [25].

When the activity of a catalyst is lowered below a critical point due to green oil formation, the catalyst undergoes regeneration at high temperatures in air to remove green oil from the catalyst in a commercial process. During regeneration, Pd particles are usually sintered due to the high temperatures, leading to the reduced hydrogenation activity of Pd catalyst. The Si species modifying the Pd surface in this study would be expected to reduce the mobility of Pd crystallites even at high temperatures so as to retard metal sintering.

Fig. 9 shows infrared spectra of CO adsorbed on the catalysts before and after regeneration. Before regeneration, the overall spectral intensity of $Pd–Si/SiO_2$ was reduced and the band at 1995 cm^{-1}, assigned as the compressed-bridged mode [35], was significantly suppressed, as compared to those of Pd/SiO_2, due to the effective blocking of multi-coordination sites of Pd by the added Si, as explained before. Spectral changes were observed in both catalysts after regeneration. The ratio of the intensity of the CO band at 1995 cm^{-1}, corresponding to the compressed-bridged mode, to those of bands at 2094 cm^{-1}, corresponding to the linear modes, and at 1925 cm^{-1}, the isolated-bridged mode, is an index for estimating the relative fraction of multiply coordinated sites on the Pd surface. That is, the A_m/A_l ratio increases when the size of Pd crystallites grows. The ratio obtained from Fig. 9 increases from 0.23

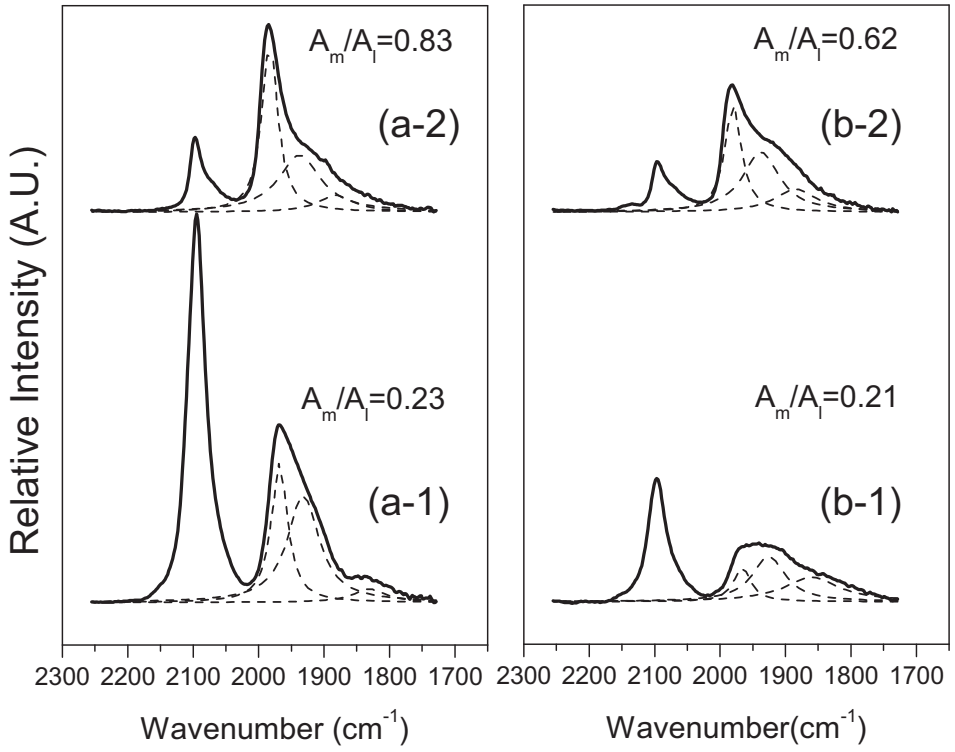

Fig. 9. Infrared spectra of CO adsorbed on the catalysts before and after the catalyst regeneration: (a) Pd/SiO_2; (b) $Pd–Si/SiO_2$: (1) fresh; (2) after regeneration [27].

to 0.83, by a factor of 3.61, on Pd/SiO_2 and from 0.21 to 0.62, by a factor of 2.95, on $Pd–Si/SiO_2$. The results indicate that sintering of Pd crystallites is retarded when the catalyst surface is modified with the Si species.

The regenerated catalysts were tested again for acetylene hydrogenation and the results are shown in Fig. 3. The initial activity of a fresh catalyst was reduced after the regeneration, but the extent of the activity decrease was smaller with $Pd–Si/SiO_2$ than with Pd/SiO_2 [27]. It is significant that Pd/SiO_2 was deactivated at faster rates after catalyst regeneration, while $Pd–Si/SiO_2$ maintained almost the same deactivation rate even after regeneration. Accordingly, the added Si retarded catalyst deactivation even after catalyst regeneration.

3. Pd catalysts modified with metal oxides showing an SMSI behavior

3.1. TiO_2-modified Pd catalyst

3.1.1. SMSI behavior of TiO_2-modified Pd catalyst

TiO_2 was selected as a potential promoter of Pd because it interacted strongly with Pd when used as a support, particularly after reduction at high temperatures like 500 °C. The strong metal–support interaction (SMSI) has been observed in vast number catalysts supported on reducible metal oxides, including TiO_2 [43,44]. The SMSI phenomenon induces the geometric modification of the metal surface with partially reduced metal oxides that are used as supports [45–50], and it also induces the electronic modification of the metal through an electron transfer between the support and the dispersed metals [51,52]. The similarity between the role of selectivity promoters of Pd catalysts in acetylene hydrogenation described in the previous section and the role of reducible oxide supports in the SMSI phenomenon encouraged us to investigate the use of TiO_2 as a promoter, instead of support, for the acetylene hydrogenation catalyst.

The typical result of SMSI is a significant reduction of gas adsorption, as has been reported previously [43,44]. Therefore, we first investigated H_2 and CO adsorption behavior of TiO_2-containing catalysts to investigate if TiO_2, added as a promoter also induced SMSI phenomenon with Pd. Three different catalysts, i.e., Pd/SiO_2, Pd/TiO_2 and TiO_2-added Pd/SiO_2 ($Pd–Ti/SiO_2$), were prepared as reported previously [14]. The H_2 and CO adsorption experiments on these catalysts were performed at two different reduction temperatures, i.e., 500 °C and 300 °C, which are typical temperatures for either inducing or not inducing SMSI, respectively. In Table 1, the H/Pd and CO/Pd ratios of Pd/SiO_2 are lowered by nearly the same extent when the reduction temperature is raised from 300 to 500 °C, which is obviously due to the sintering of Pd particles during high temperature reduction, as explained earlier. The Pd/TiO_2 catalyst reduced at 300 °C ($Pd/TiO_2/300$) adsorbs smaller amounts of H_2 and CO than does $Pd/SiO_2/300$, indicating that the Pd dispersion is relatively poor when TiO_2 instead of SiO_2 is used as a support. When Pd/TiO_2 is reduced at 500 °C ($Pd/TiO_2/500$), both H_2 and CO adsorption is significantly suppressed, which is the well-known SMSI phenomenon, as has been reported previously [43,44]. $Pd–Ti/SiO_2$ showed similar gas absorption behavior compared to

Table 1
H_2 and CO adsorption data for sample catalysts reduced at different temperatures [14].

Catalysts	H/Pd	CO/Pd	A_m/A_l [a]	H/Pd[b]
$Pd/SiO_2/300$[c]	0.79	0.76	2.5	0.45
$Pd/SiO_2/500$	0.54	0.52	4.5	0.38
$Pd/TiO_2/300$	0.34	0.47	–	–
$Pd/TiO_2/500$	0.02	0.01	–	–
$Pd–Ti/SiO_2/300$	0.61	0.63	2.7	0.58
$Pd–Ti/SiO_2/500$	0.19	0.17	1.6	0.25

[a] The area ratio of the multiply bound to the linearly bound CO bands.
[b] The H/Pd ratio for the catalyst oxidized in O_2 at 300 °C and subsequently reduced at different temperatures.
[c] 1 wt.% Pd/SiO_2 reduced at 300 °C.

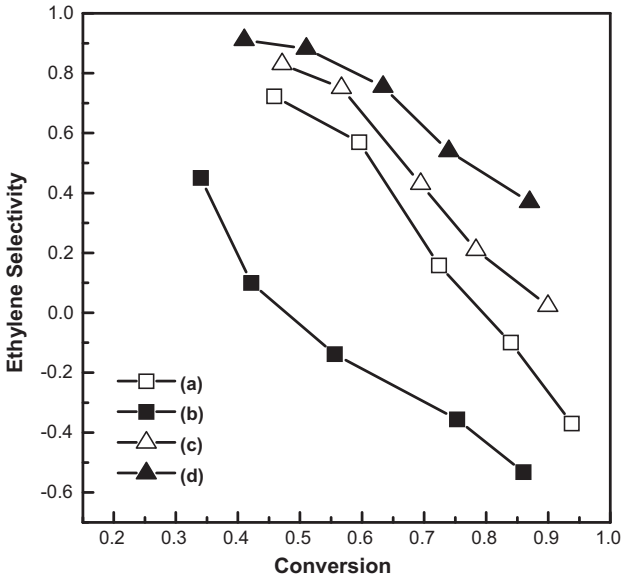

Fig. 10. Changes in ethylene selectivity with conversion in acetylene hydrogenation on catalysts containing different amounts of TiO_2: (a) $Pd/SiO_2/300$; (b) $Pd/SiO_2/500$; (c) $Pd–Ti/SiO_2/300$; (d) $Pd–Ti/SiO_2/500$ [14].

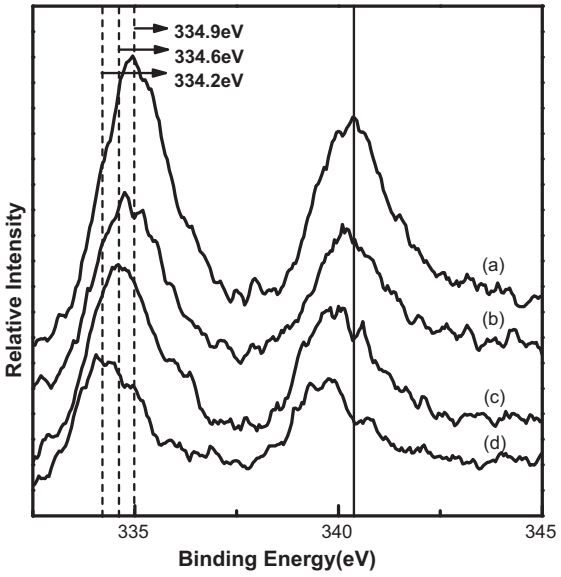

Fig. 11. XPS of Pd $3d_{5/2}$ for sample catalysts: (a) $Pd/SiO_2/300$; (b) $Pd–Ti/SiO_2/300$; (c) $Pd–Ti/SiO_2/500$; (d) $Pd–10Ti/SiO_2/500$ [14].

that of Pd/TiO_2, that is, H_2 and CO chemisorption was remarkably suppressed after high temperature reduction ($Pd–Ti/SiO_2/500$), indicating that SMSI still occurred when TiO_2 was used as a promoter rather than a support, although the extent was not as large as in the latter. Reversible behavior of gas adsorption upon oxidation followed by reduction at different temperatures, which was an additional evidence of SMSI phenomenon, was also observed on $Pd–Ti/SiO_2$ [14].

3.1.2. Catalytic performance of TiO_2-added Pd catalyst

Typical ethylene selectivity data obtained using Pd/SiO_2 and Pd/TiO_2 catalysts over a wide range of acetylene conversions under the same reaction conditions are shown in Fig. S1 (Supplementary Information). Both the conversion and selectivity of Pd/SiO_2 were lowered as the reduction temperature was raised from 300 °C to 500 °C due to the sintering of Pd particles at 500 °C. $Pd/TiO_2/300$ exhibited lower conversions than $Pd/SiO_2/300$ due to the lower Pd dispersion on TiO_2 than on SiO_2. The activity of Pd/TiO_2 was further lowered after reduction at 500 °C because the Pd surface was covered with a large amount of Ti species, which was a characteristic feature of the SMSI phenomenon [43,44]. The TiO_2-added catalyst, $Pd–Ti/SiO_2$, also lost its activity after reduction at 500 °C as shown in Fig. 10, however the activity loss was much smaller than that in the case of Pd/TiO_2. The selectivity curve shifted upward when the catalyst was reduced at 500 °C ($Pd–Ti/SiO_2/500$), which clearly demonstrated the advantage of TiO_2 as a selectivity promoter. The enhanced performance of the $Pd–Ti/SiO_2$ catalyst was achieved because TiO_2 was added to the well-dispersed Pd/SiO_2. With Pd/TiO_2, the performance improvement was limited due to the poor dispersion of Pd on TiO_2. There was an optimum Ti/Pd ratio for maximum selectivity, apparently because the selectivity promotion by added TiO_2 was eventually retarded when a large portion of the Pd surface was decorated with Ti species. The maximum selectivity was obtained when the Ti/Pd ratio was between 1.0 and 2.0 [14].

To understand the origin of selectivity promotion by added TiO_2, we investigated the electronic and geometric structure changes of Pd/SiO_2 upon TiO_2 addition at various reduction temperatures. Fig. 11 shows XPS results of the catalysts, showing that the peak representing the binding energy of Pd $3d_{5/2}$ electrons appeared almost at the same position for $Pd/SiO_2/300$ and $Pd–Ti/SiO_2/300$, but was shifted to a lower binding energy for $Pd–Ti/SiO_2/500$. These results indicate that there was no charge transfer from the added TiO_2 to Pd just by the TiO_2 addition, rather, the charge transfer was induced by high temperature reduction at 500 °C [53–56]. The fact that the peak shift was even greater for $Pd–10Ti/SiO_2/500$, which contained larger amounts of Ti, further supported the idea that the Pd was electronically modified by TiO_2 after high temperature reduction.

To further study the surface geometric properties of $Pd–Ti/SiO_2$, IR spectra of CO adsorbed on the catalyst were obtained and the results compared with those observed for Pd/SiO_2, as shown in Fig. 12. The CO band intensity on $Pd–Ti/SiO_2/300$ was lower than that on $Pd/SiO_2/300$, indicating a partial coverage of the Pd surface with the Ti species. It should be noted that the intensity of the 1870–1890 cm^{-1} band representing the tri-coordinated CO adsorption was lowered upon TiO_2 addition, indicating that the added Ti species preferentially blocked the sites with three adjacent Pd atoms. The intensity of the CO bands on $Pd–Ti/SiO_2$

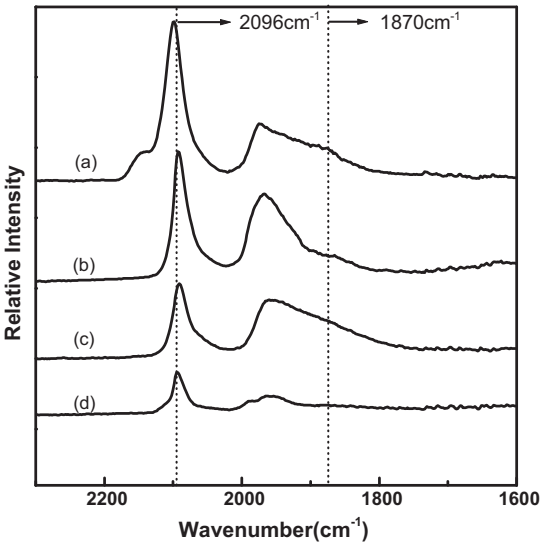

Fig. 12. Infrared spectra of CO adsorbed on sample catalysts: (a) $Pd/SiO_2/300$; (b) $Pd–Ti/SiO_2/300$; (c) $Pd/SiO_2/500$; (d) $Pd–Ti/SiO_2/500$ [14].

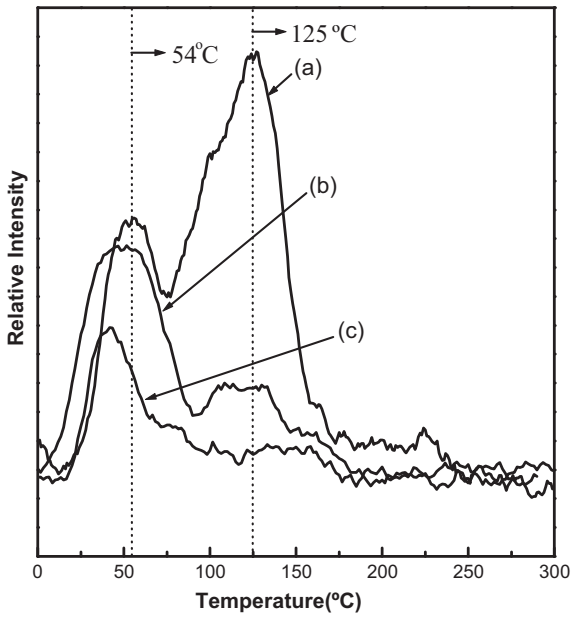

Fig. 13. TPD of ethylene from sample catalysts: (a) $Pd/SiO_2/300$; (b) $Pd–Ti/SiO_2/300$; (c) $Pd–Ti/SiO_2/500$ [14].

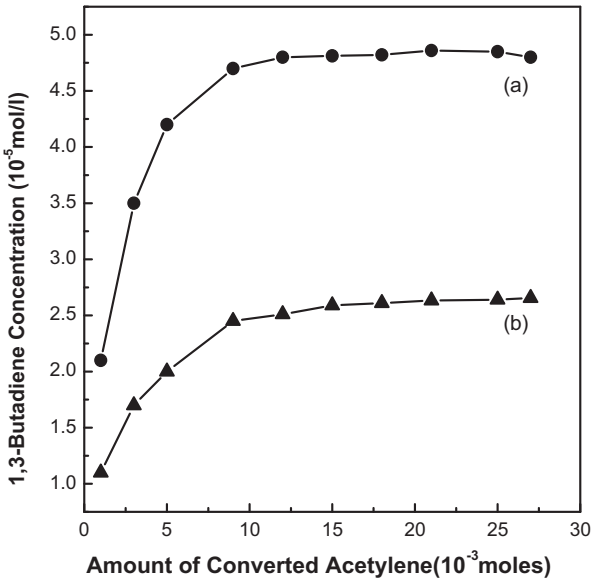

Fig. 14. The concentration of 1,3-butadiene measured in the exit streamof reactor containing sample catalysts (H_2/acetylene = 1, T = 70 °C): (a) $Pd/SiO_2/300$; (b) $Pd–Ti/SiO_2/500$ [14].

was significantly suppressed when the catalyst was reduced at 500 °C ($Pd–Ti/SiO_2/500$). This result was not due to the sintering of Pd particles, as observed with $Pd/SiO_2/500$, because the ratio of the multiply bound to the linearly bound bands, A_m/A_l, of $Pd–Ti/SiO_2/500$ decreased from 2.7 to 1.6, which was a trend opposite to the one expected in the case of Pd sintering. The concurrent suppression of the CO absorption intensity and a decrease in the A_m/A_l ratio was possible only when the Ti species added to the catalyst covered the Pd surface, thus blocking the multi-coordination sites of Pd on $Pd–Ti/SiO_2/500$ [14].

Fig. 13 shows that peaks of ethylene-TPD from the Pd surface appear at different temperatures depending on the characteristic modes of ethylene adsorption on the Pd surface. $Pd/SiO_2/300$ showed two major peaks. As explained in Section 2.3, the peak at 54 °C represents weakly adsorbed π-bonded ethylene, which desorbs without decomposition. The peak at 125 °C represents di-σ-bonded ethylene, which undergoes decomposition and recombination with hydrogen to produce ethylene and ethane [40]. Upon TiO_2 addition ($Pd–Ti/SiO_2/300$), the peak intensity at 125 °C was remarkably reduced and the low temperature peak was slightly shifted to lower temperatures. The trend became more evident for $Pd–Ti/SiO_2/500$. The ethylene-TPD results were in agreement with the IR and XPS results (Figs. 11 and 12) in the following aspects. The Pd surface was modified geometrically by the Ti species, as confirmed by the CO-IR spectra, such that the decomposition of ethylene was suppressed. Charge transfer from the Ti species to Pd further reduced the adsorption strength of weakly adsorbed ethylene, thus facilitating Path II in the reaction mechanism of acetylene hydrogenation (Fig. 1), thus increasing the ethylene selectivity. The TPD results in this study were consistent with those previously reported by Briggs et al. [57], who also observed a reduction in the strength of ethylene adsorption on Pt/TiO_2, upon high temperature reduction. They attributed the weakening of the adsorption strength to interactions between Pt and partially reduced titania.

3.1.3. *Catalyst deactivation behavior of TiO_2-modified Pd catalyst*

As inferred from the surface structure changes of Pd catalyst upon TiO_2 addition, the TiO_2-modified Pd catalyst exhibited enhanced performance in catalyst deactivation similar to the case of the Si-modified catalyst.

Fig. 14 shows the concentration of 1,3-butadiene observed in the exit stream of the reactor containing either $Pd/SiO_2/300$ or $Pd–Ti/SiO_2/500$. 1,3-Butadiene, which is produced by the dimerization of C_2 species, is proposed as a precursor of green oil formation and is preferentially produced, especially when acetylene is adsorbed on neighboring Pd sites. Fig. 14 shows that 1,3-butadiene is produced in smaller amounts on $Pd–Ti/SiO_2/500$ than on $Pd/SiO_2/300$. Because 1,3-butadiene is formed on multi-coordination sites of Pd, which can accommodate adjacent C_2 species, the above result suggests that large ensembles of Pd are effectively blocked by the added Ti species, thus the production of green oil is suppressed.

Fig. 15 shows the deactivation rates of $Pd/SiO_2/300$ and $Pd–Ti/SiO_2/500$ before and after regeneration. It is obvious that

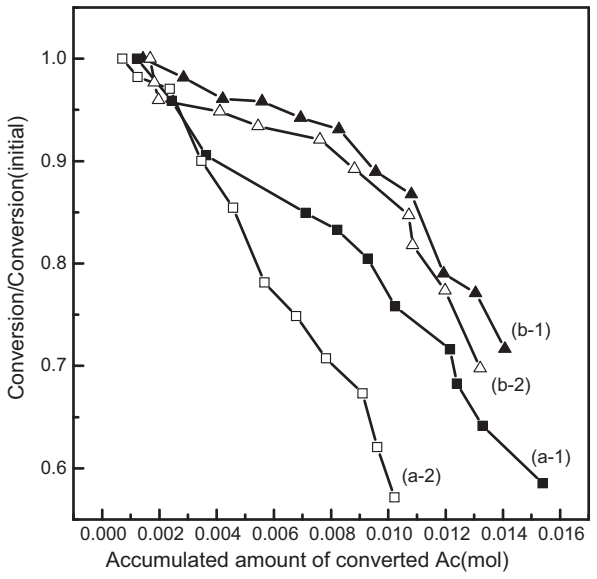

Fig. 15. Deactivation of catalysts, before and after regeneration, with accumulated amounts of converted acetylene (regenerating conditions: O_2 = 20 cm^3/min, temperature = 600 °C for 2 h): (a) $Pd/SiO_2/300$; (b) $Pd–Ti/SiO_2/500$: (1) fresh; (2) after regeneration [29].

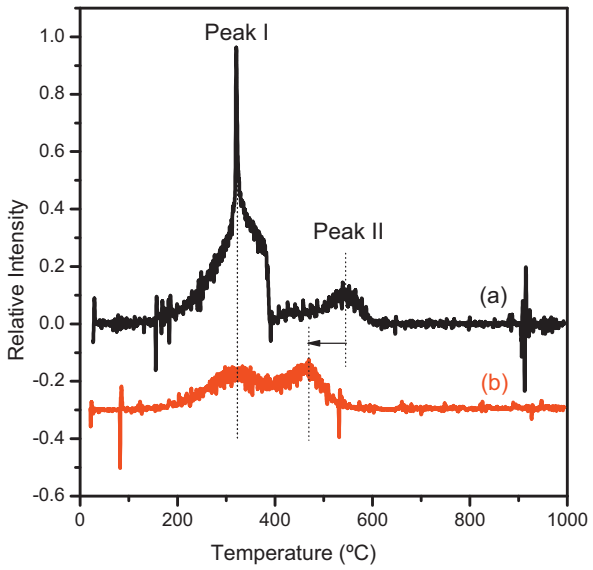

Fig. 16. Differential thermogravimetric analysis of used catalysts in air: (a) $Pd/SiO_2/300$; (b) $Pd–Ti/SiO_2/500$ [29].

$Pd–Ti/SiO_2/500$ undergoes slower deactivation than $Pd/SiO_2/300$, as expected from the 1,3-butadiene analysis. Catalysts used for converting the same amounts of acetylene were regenerated in air at 600 °C, before being reduced and used again for the deactivation tests. In the case of $Pd/SiO_2/300$, the activity decreased at a much faster rate after the regeneration, which was obviously due to the sintering of Pd crystallites caused by high temperature regeneration. On the other hand, the activity of regenerated $Pd–Ti/SiO_2/500$ decreased nearly at the same rates as were observed before the regeneration, indicating that added TiO_2 suppressed the sintering of Pd crystallites.

Fig. 16 shows the results of a differential thermogravimetric analysis (DTGA) obtained from the TGA curves, which can be deconvoluted into two major peaks: Peak I (300–370 °C), representing coke produced on and in the vicinity of the Pd, and Peak II (400–600 °C), representing graphite-like coke present on the support [23]. When the Pd catalyst is modified with TiO_2, the area of Peak I is significantly reduced, indicating that the formation of green oil on and in the vicinity of Pd is suppressed, and the location of Peak II is shifted to lower temperatures, indicating that green-oil produced on the support can be removed at relatively low temperatures.

Fig. 17 shows IR spectra of CO adsorbed on the catalysts before and after regeneration. After regeneration, the A_m/A_l ratio increased from 2.6 to 4.9 for $Pd/SiO_2/300$, due to the sintering of Pd crystallites, but the ratio increased only slightly, from 1.6 to 1.9, for $Pd–Ti/SiO_2/500$, indicating that the sintering of Pd crystallites was suppressed by the added TiO_2.

The above properties of $Pd–Ti/SiO_2/500$ can be correlated with the reaction paths for acetylene hydrogenation (Fig. 1), such that the selectivity improvement of the catalyst is explained based on either the promotion or the suppression of individual paths. Path IV is suppressed when the Pd surface is decorated with, and consequently the neighboring Pd sites are blocked by, Ti species. This explanation is consistent with the observation that 1,3-butadiene is produced in smaller amounts on $Pd–Ti/SiO_2/500$ than on $Pd/SiO_2/300$. The significant suppression of H_2 adsorption on $Pd–Ti/SiO_2/500$ will suppress both Paths I and III. In fact, this situation is the same as using low H_2/acetylene ratios in the feed of acetylene hydrogenation, which suppresses Path III more than Path I and consequently improves ethylene selectivity [58]. On the other hand, the weakening of ethylene adsorption on

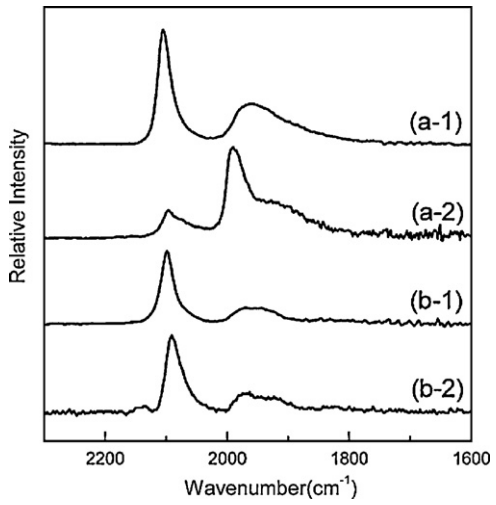

Fig. 17. Infrared spectra of CO adsorbed on the catalysts before and after catalyst regeneration: (a) $Pd/SiO_2/300$; (b) $Pd–Ti/SiO_2/500$: (1) fresh; (2) after regeneration [29].

$Pd–Ti/SiO_2/500$ obviously contributes to the ethylene selectivity because it promotes Path II, leading to the production of gaseous ethylene. Accordingly, the surface properties of $Pd–Ti/SiO_2/500$ agree with the trends that the reaction paths of acetylene hydrogenation would be expected to follow, allowing for the ethylene selectivity.

3.2. Other SMSI promoters

To investigate if the enhanced performance of Pd catalyst by the SMSI effect was due to a unique property of the TiO_2, other oxides, i.e., Nb_2O_5 and La_2O_3, were also investigated [30]. Nb_2O_5 was selected because they are reducible at relatively low temperatures compared to TiO_2 [43]. On the other hand, La_2O_3 was selected because it was difficult to reduce, being sometimes referred to as a non-reducible oxide [59]. $Pd–X/SiO_2$ (X = Ti, Nb, La) were prepared by a method reported previously [26].

Fig. 18 shows the TPR profiles for various catalysts, where the first peak (50–170 °C) represents the reduction of PdO and the second peak (above 200 °C) represents the reduction of added oxides [60–62]. The extent of interaction of Pd with the added oxides, as estimated from the shift in the first peak, was the smallest for

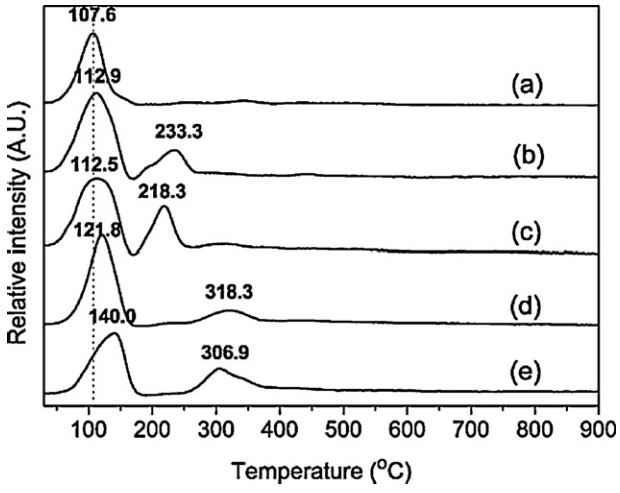

Fig. 18. TPR profiles for sample catalysts: (a) Pd/SiO_2; (b) $Pd–1Ti/SiO_2$; (c) $Pd–1Nb/SiO_2$; (d) $Pd–1La/SiO_2$; (e) $Pd–3La/SiO_2$ [30].

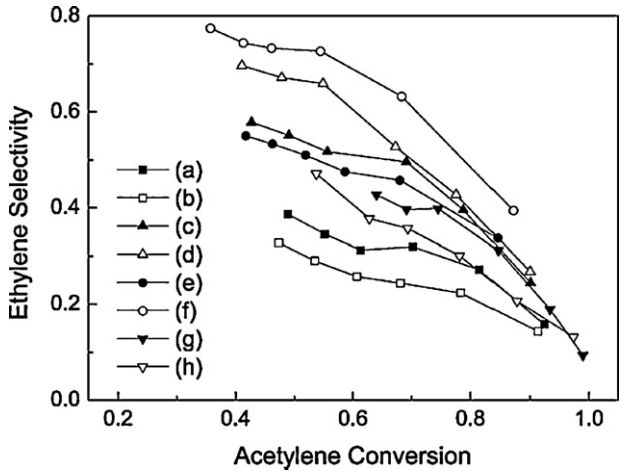

Fig. 19. Changes in the ethylene selectivity with conversion in acetylene hydrogenation for different sample catalysts (H_2/acetylene = 2, reduction temperature = 300 °C or 500 °C, reaction temperature = 60 °C): (a) Pd/300; (b) Pd/500; (c) Pd–Ti/300; (d) Pd–Ti/500; (e) Pd–La/300; (f) Pd–La/500; (g) Pd–Nb/300; (h) Pd–Nb/500 [30].

Pd–Nb/SiO_2 and the largest for Pd–La/SiO_2, which was the same sequence as for the reducibility of the oxides, which was estimated from the position of the second peak.

Fig. 19 shows the ethylene selectivity versus acetylene conversion for a reaction at 60 °C using catalyst samples reduced at different temperatures. Among three oxides added as promoters, La_2O_3 reduced at 500 °C showed the largest promotion of the ethylene selectivity, followed by TiO_2 and Nb_2O_5, which was the same sequence as that for the extent of interaction between oxides and Pd. It is noteworthy that Pd–Nb/SiO_2 had an additional activity for hydrogenation compared to Pd/SiO_2. This result was obtained because Nb_2O_5 had additional hydrogenation activity due to the facilitated adsorption of hydrogen, as reported in the literature [63–65]. The additional hydrogenation activity of Nb_2O_5 also contributed to the production of relatively volatile green-oils and eventually to remarkably low rates of catalyst deactivation [30]. The selectivity of Pd–Nb/SiO_2 decreased after reduction at 500 °C instead of at 300 °C, unlike the other SMSI oxides. On the other hand, the selectivity of Pd–La/SiO_2 increased after reduction at 500 °C (Pd–La/500) instead of at 300 °C. Considering the characteristic behaviors of La_2O_3- and Nb_2O_5-added catalysts, it was proposed that the former catalysts were advantageous for use in acetylene hydrogenation at high temperatures and the latter at low temperatures [30].

For an SMSI between TiO_2 and Pd to arise, the catalyst must be reduced at high temperatures, e.g. 500 °C [43,44]. However, the maximum temperature tolerable in most industrial reactors for acetylene hydrogenation is only about 300 °C, which is too low to induce the SMSI effect. Accordingly, improvements in ethylene selectivity by the use of added TiO_2 species is limited by industrial conditions. In this respect, a new catalyst, which exhibits an SMSI phenomenon even after reduction at low temperatures, hopefully below 300 °C, would be highly desirable for industrial applications.

We added potassium to TiO_2-modified Pd catalyst to lower the temperature required for inducing the SMSI effect, because potassium is known to interact with TiO_2 to form potassium titanates (e.g. K_2TiO_3, $K_2Ti_2O_5$, $K_2Ti_4O_9$, and $K_2Ti_6O_{13}$), all of which exhibit melting points that are significantly lower than that of TiO_2 [66].

As shown in Fig. S2 (Supplementary Information), potassium itself had a promotional effect on the ethylene selectivity of Pd/SiO_2 reduced at 300 °C (Pd–K/300), presumably due to the electronic effect of K, as observed in our previous work [28] and also proposed for other similar systems [12]. However, the extent of selectivity improvement by only the added K was not as significant as that obtained by added TiO_2. It is noteworthy that Pd–Ti/SiO_2 containing a small amount of K, e.g., at a K/Pd atomic ratio of 0.1 (Pd–Ti–0.1K/300), showed much improved ethylene selectivity even after reduction at 300 °C, which was not sufficiently high to induce a strong interaction between Pd and the TiO_2 as in the case of K-free Pd–Ti/SiO_2. The above results indicate that potassium addition had an effect on lowering the temperature inducing the SMSI effect on the TiO_2-modified Pd catalyst.

4. Characteristic deactivation behavior of Pd catalyst in acetylene hydrogenation

4.1. Green-oil precursor

Among C_4 species produced from dissociatively adsorbed acetylene, 1,3-butadiene has been proposed as the major precursor of green oil due to its volatility and easiness for polymerization [34,67,68]. To clarify the green oil precursor in acetylene hydrogenation, we investigated the deactivation characteristics of Pd/SiO_2 in acetylene hydrogenation by simultaneously monitoring changes in the deactivation rates, catalyst weight, and the amounts of C_4 species produced in the reaction.

Fig. 20(a) shows simultaneous changes in the activity and weight of the catalyst during the deactivation process. The activity decreased together with an increase in catalyst weight, suggesting that the accumulation of green oil was a major reason for the catalyst deactivation [69]. The mol fractions of all C_4 species formed during the deactivation process were measured, as shown in Fig. 20(b). The amounts of all butene species (1-butene, trans-2-butene, and cis-2-butene) decreased with the amounts of converted acetylene, indicating that butene species were not the precursors of green-oil. On the other hand, the amounts of 1,3-butadiene started to increase when the amounts of converted acetylene were larger than 0.020 mol, but eventually decreased in the later stage after reaching a maximum at ca. 0.025 mol. To further investigate the correlation between 1,3-butadiene and green-oil formation, we compared the DTGA results, which represented the rates of green-oil formation, with the amounts of 1,3-butadiene produced in the reaction, as shown in Fig. 20(c). The results demonstrate a close similarity between the two parameters, that is, the rate of green-oil formation is proportional to that of 1,3-butadiene formation [67,68].

The amounts of 1,3-butadiene produced in the deactivation process changed, exhibiting a maximum with catalyst deactivation. This result can be explained based on the reaction mechanism proposed in Fig. 21. Since 1,3-butadiene was an intermediate in the sequential reaction process for converting acetylene to either butenes (Step 4) or green oil (Step 5), the amounts of 1,3-butadiene produced were influenced by relative rates of Step 3, producing 1,3-butadiene, and Steps 4 and 5, consuming 1,3-butadiene. At an early stage of catalyst deactivation, the rates of butadiene hydrogenation (Step 4) were retarded to a greater extent than those for acetylene dimerization (Step 3). This result was obtained because Step 4 involved hydrogenation, which was directly affected by catalyst deactivation, while Step 3 involved the dimerization of acetylene, which was less sensitive to catalyst deactivation since the acetylene was more strongly adsorbed to the catalyst than hydrogen [12,13]. At the late stage of the deactivation, both Steps 3 and 4 were significantly retarded due to a decrease in the Pd surface available for either adsorption of acetylene and hydrogen and consequently the production of 1,3-butadiene was also retarded in parallel with catalyst activity.

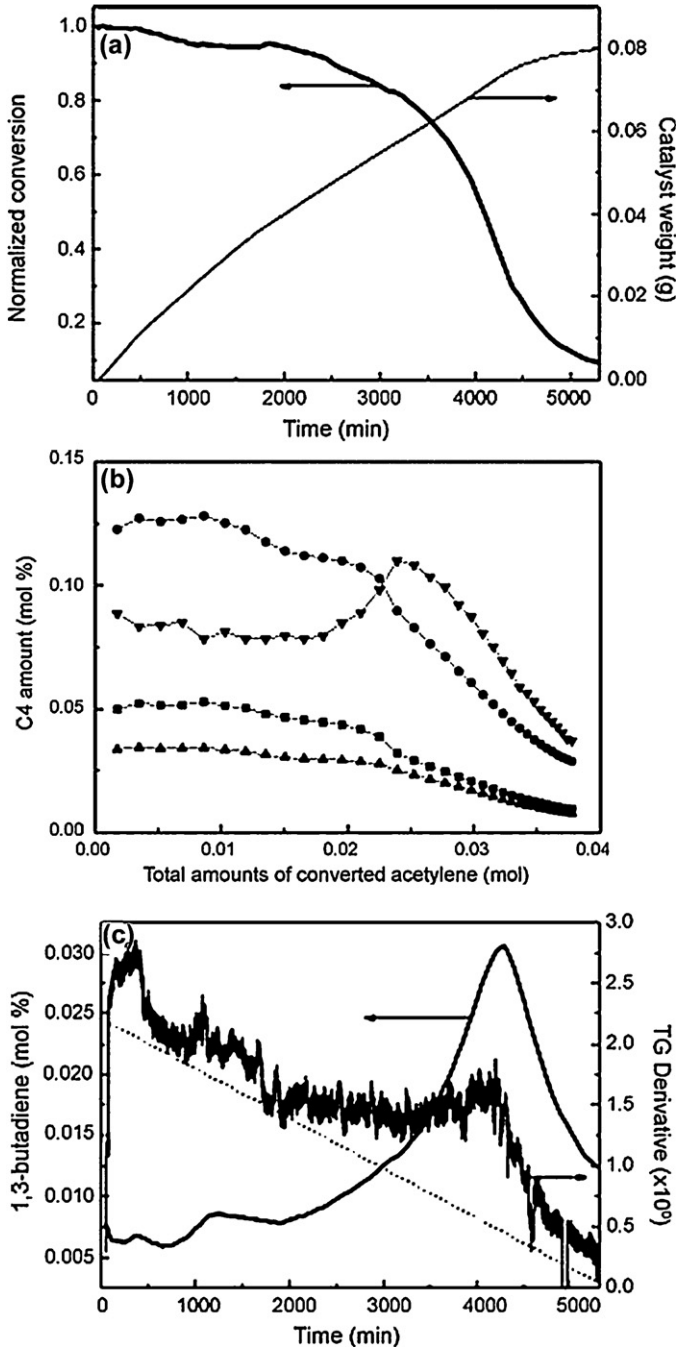

Fig. 20. (a) Changes in the amount of C_4 products as a function of the total amounts of converted acetylene: 1-butene (●); trans-2-butene (■); cis-2-butene (▲); 1,3-butadiene (▼). Changes in the activity, catalyst weight, and the amount of produced 1,3-butadiene with process time, obtained by simultaneous TG/reaction experiments (H_2/acetylene = 1, reaction temperature = 70 °C): (b) the activity (normalized to initial conversion) and catalyst weight; (c) the amount of produced 1,3-butadiene and gradients in the TG curve [69].

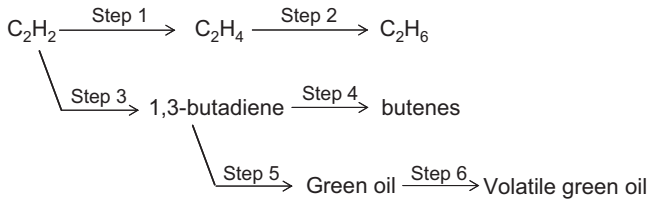

Fig. 21. Reaction steps involved in acetylene hydrogenation process [69].

4.2. Self-regenerative behavior of Pd catalyst in the deactivation process

The H_2/acetylene ratio also plays an important role in the catalyst deactivation [24,70]. The catalyst deactivation was retarded when the reaction was conducted at a high H_2/acetylene ratio, as shown in Fig. 22, obviously because green-oil formation was suppressed due to an increased supply of hydrogen [24]. In addition, the catalyst exhibited a very interesting characteristic pattern, i.e. self-regenerative behavior, at the early stage of catalyst deactivation and it was more distinct when the deactivation was performed at high H_2/acetylene ratios. The activity was recovered

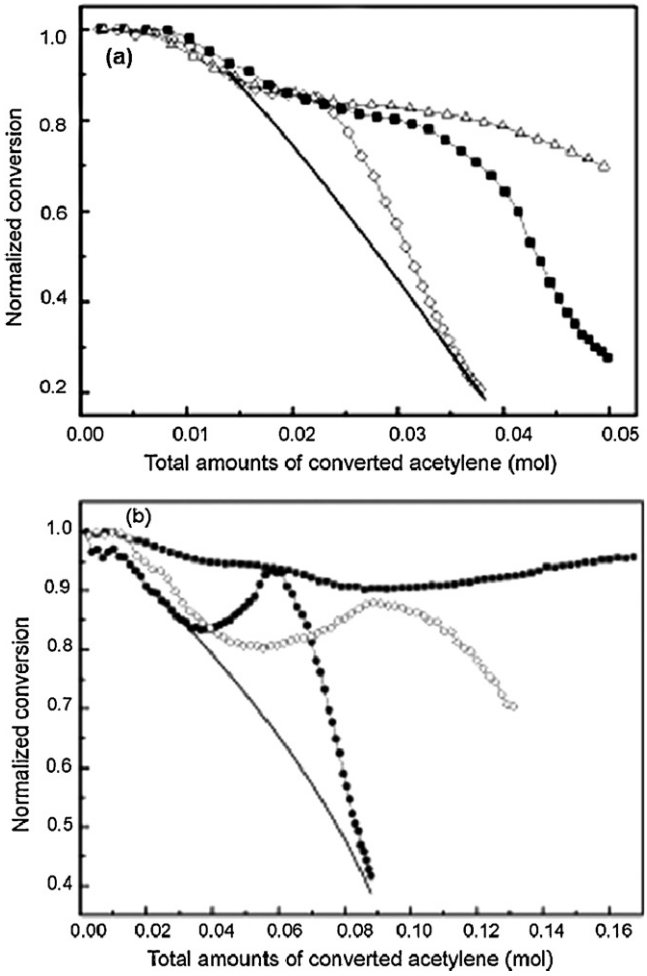

Fig. 22. Changes in the catalyst activity (normalized conversion) as a function of the total amounts of converted acetylene. (a) H_2/acetylene = 1: Pd/110 (△); Pd/90 (■); Pd/70 (◊), (b) H_2/acetylene = 2: Pd/90 (■); Pd/70 (◊); Pd/50 (●) [69].

after the initial drop and reached a maximum before it significantly decreased in the later stage. This phenomenon was also observed in butene production, as shown in Fig. S3, which changed in parallel with catalyst activity. The self-regenerative behavior in the early stage of catalyst deactivation suggests that two factors that contributed to the activity in opposite ways were involved in the deactivation process. One was the accumulation of green oil on the catalyst surface, which lowered its activity. The other, proposed for the first time in this study, involved the production of a specific type of green-oil, which had the capability to store and spillover hydrogen, and it consequently contributed to the additional hydrogenation activity, as revealed in previous studies [8,71].

4.3. Three-stage deactivation of the Pd catalyst

According to Fig. 23, which was obtained by catalyst-deactivation studies made using Pd/SiO_2 and $Pd–0.05Ag/SiO_2$ [72], the deactivation of Pd/SiO_2 proceeded in three stages. That is, the activity remained nearly constant when the accumulated amounts of converted acetylene were smaller than 0.014 mol (Period I). The activity decreased slightly during the intermediate period (Period II), and finally decreased significantly when the accumulated amounts of converted acetylene were larger than 0.030 mol (Period III). The properties of green oil species formed on Pd/SiO_2 and $Pd–0.5Ag/SiO_2$ during the above three stages of deactivation were investigated and correlated with the deactivation behaviors.

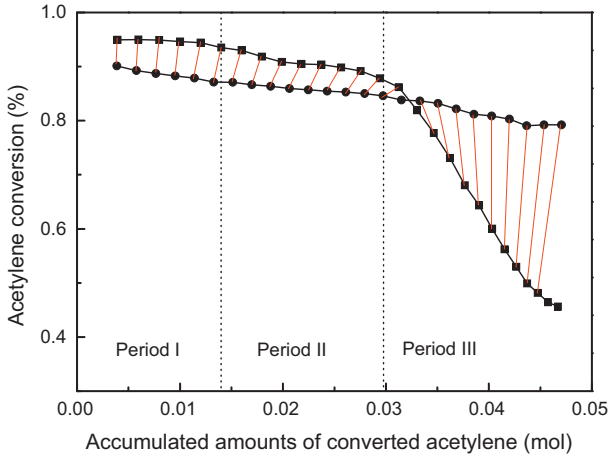

Fig. 23. Changes in the catalytic activity as a function of the accumulated amounts of converted acetylene on Pd/SiO_2 (■) and $Pd–0.5Ag/SiO_2$ (●) [72].

Fig. 24 shows the amounts of green oil deposited on the catalysts obtained by EA and TGA as a function of acetylene conversion during deactivation, and Fig. 25 shows DTGA results of both catalysts after use for different periods of time. The deactivation of Pd/SiO_2 in the acetylene hydrogenation proceeded in three stages. In Period I, large amounts of green oil were deposited (about 34 wt.%) onto the catalyst but the activity only slightly decreased by 2%. As the deactivation proceeded (Period II), the rates of green-oil deposition became slightly lower than those during the initial period. In the later stage of the process (Period III), the activity drastically decreased (from 88% to 46%) even though the amount of green oil only slightly increased (5–10 wt.%). This three-stage deactivation behavior of Pd/SiO_2 can be explained by the DTGA results shown in Fig. 25.

As explained in Section 2.4, peaks observed below 300 °C (Peak I), between 300 °C and 500 °C (Peak II), and above 500 °C (Peak III) represent heavy hydrocarbons adsorbed onto the catalyst surface and absorbed into the catalyst pores, green oil on or in the vicinity of Pd, and green oil deposited on the support, respectively [23]. Based on the above assignments of green-oil formed on the catalyst, the results in Figs. 23–25 can be explained as follows. During Period I, large amounts of green oil were deposited on or in the vicinity of the Pd surface (represented by Peak II in Fig. 25), but the catalytic activity decreased only slightly, indicating that

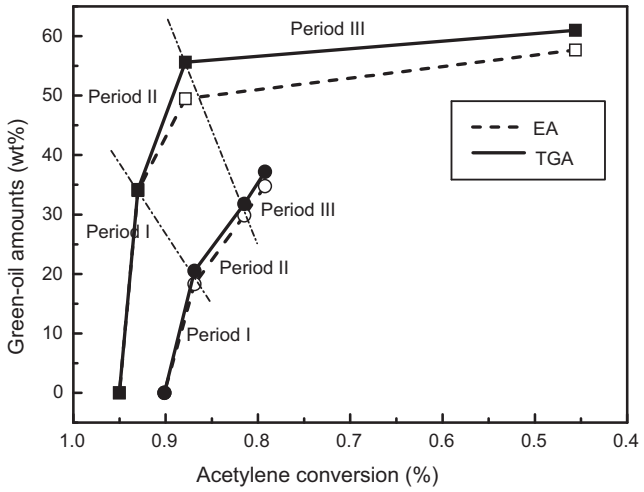

Fig. 24. The amounts of green oil deposited on Pd/SiO_2 (■) and $Pd–0.5Ag/SiO_2$ (●), analyzed by TGA (—) and EA (– –) [72].

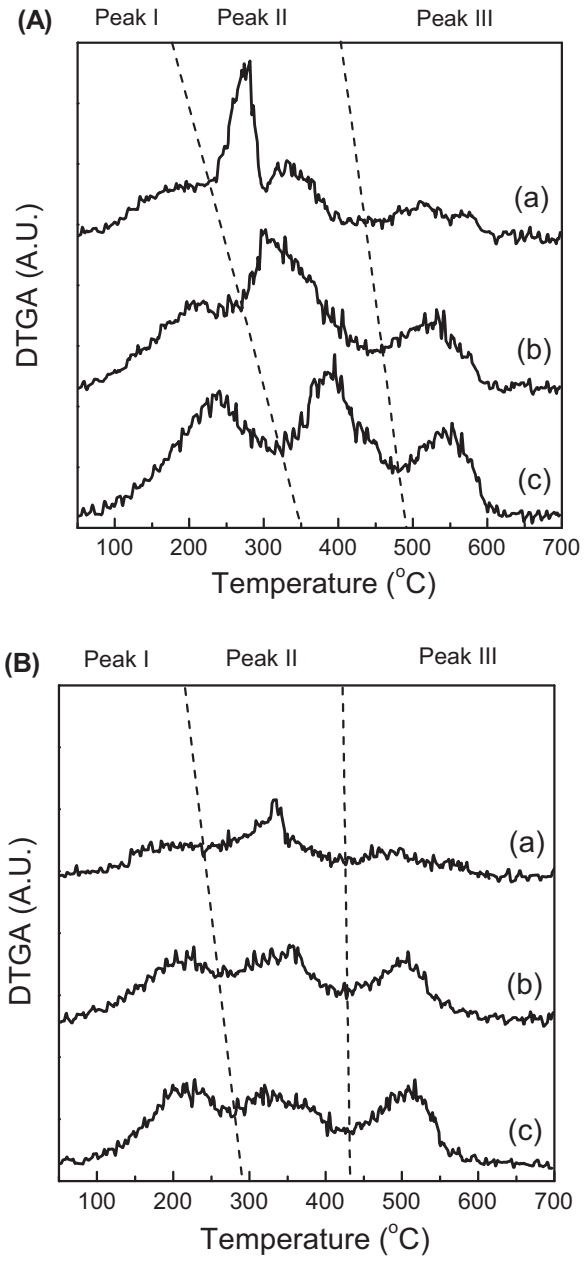

Fig. 25. DTGA of (A) Pd/SiO_2 and (B) $Pd–0.5Ag/SiO_2$ after use for different periods: (a) Period I; (b) Period II; (c) Period [72].

the green-oil formed during the initial deactivation period was not detrimental to the activity. The hydrogen transfer mechanism proposed by others [73,74] can explain the above results. That is, acetylenic species adsorbed on the carbonaceous overlayer, which covers the Pd surface, can be hydrogenated to ethylene by reaction with hydrogen transferred through the carbonaceous overlayer. Consequently, the rate of acetylene hydrogenation was not affected by the large amounts of green-oil deposited in the initial stage (Period I). In the middle period of the reaction (Period II), green-oil, which was initially deposited on or in the vicinity of the Pd surface (Peak II), was polymerized to a heavier species, as evidenced by the peak shift to higher temperatures. The polymerized species spilled over to the support (Peak III) and catalyst pores (Peak I), thus contributing to a decrease in the activity of Pd/SiO_2. In the later stage of deactivation (Period III), catalytic activity drastically decreased because catalyst pores were blocked by the accumulated green oil (Peak I) and hydrogen diffusion was limited in the thick film of the relatively heavy green oil.

The deactivation was significantly retarded when Ag was added to Pd/SiO_2. The amount of green oil deposited on the Pd surface (Peak II) was much smaller than that deposited on Pd/SiO_2. Furthermore, the amounts of green oil adsorbed onto the catalyst surface (Peak I) and deposited on the support (Peak III) were relatively large in Period II and III, whereas those on the Pd surface (Peak II) were small. These results indicate that green oil, primarily formed on the Pd surface in small amounts, easily moved to the support in the case of $Pd–Ag/SiO_2$. Consequently, the final stage of deactivation (Period III), due to diffusion limitation in catalyst pores, was not observed with $Pd–Ag/SiO_2$ during the reaction period of this study. Ag is well known to modify Pd electronically to facilitate the desorption of 1,3-butadiene from the Pd surface [6]. Consequently, green oil that formed on $Pd–Ag/SiO_2$ became more volatile and mobile than that formed on Pd/SiO_2, leading to a remarkable reduction of catalyst deactivation in acetylene hydrogenation.

5. Structure sensitivity of ethylene selectivity

5.1. Adding Ag or Cu promoter via a surface redox method

As indicated above, the ethylene selectivity of Pd depended on the relative fractions of different Pd surface structures, as monitored by the IR of the linear-bound, or multi-bound, CO species on the catalyst [13,14,25,26,30]. This aspect of ethylene selectivity was further investigated using Pd–Ag and Pd–Cu catalysts, which were prepared via a surface redox (SR) method that allowed the selective deposition of Ag and Cu onto Pd [31,32].

For the preparation of the Pd–Ag catalyst, a 0.3 g sample of 1 wt.% Pd/Al_2O_3 was first reduced in an H_2 and N_2 mixture ($H_2/N_2 = 1$) at 150 °C for 2 h, which was followed by cooling to room temperature in an N_2 flow. The pre-reduced 1 wt.% Pd/Al_2O_3 was exposed to anaqueous solution of $AgNO_3$ for 5 min, which allowed Ag ions in the solution to be reduced to metallic Ag by reaction with hydrogen that had been adsorbed onto the Pd surface during the pre-reduction step [31].

Pd–Cu catalysts were prepared in a similar manner, i.e., by exposing pre-reduced Pd/Al_2O_3 to a solution of $Cu(NO_3)_2$ [32]. In this case, hydrogen was bubbled through the solution during an exposure period of 1 h, which differed from the preparation conditions for Pd–Ag catalysts, to compensate for the low reduction potential of Cu ions compared with Ag ions. The prepared catalysts were washed with water, dried in air overnight, calcined in air at 300 °C, and finally reduced in H_2 at 150 °C prior to use in acetylene hydrogenation.

Fig. 26 compares the ethylene selectivity and the acetylene conversion obtained with catalysts containing Ag that was added either by impregnation (Pd–Ag (I)) or by SR (Pd–Ag (SR)). The selectivity was increased and the activity was decreased by the addition of Ag, which proceeded to greater extents in Pd–Ag (SR) than in Pd–Ag (I) even when smaller amounts of Ag were added to the former catalyst.

The results of TPD experiments (Fig. S4) show that ethylene was desorbed at lower temperatures from Pd–Ag (SR) than from Pd–Ag (I), which agreed with the above selectivity results. On the other hand, CO was desorbed at higher temperatures from Pd–Ag (SR) than from Pd–Ag (I), indicating that electron transfer from Ag to Pd was greater in the former catalyst. Consequently, the Pd–Ag interactions were stronger when Ag was added by SR instead of by impregnation.

The CO-IR results indicated that, besides the significant suppression of the multi-bound CO species on Pd due to the blocking of large Pd ensembles by added Ag, the linear-bound CO was also suppressed by Ag addition, particularly in Pd–Ag (SR) [31]. This

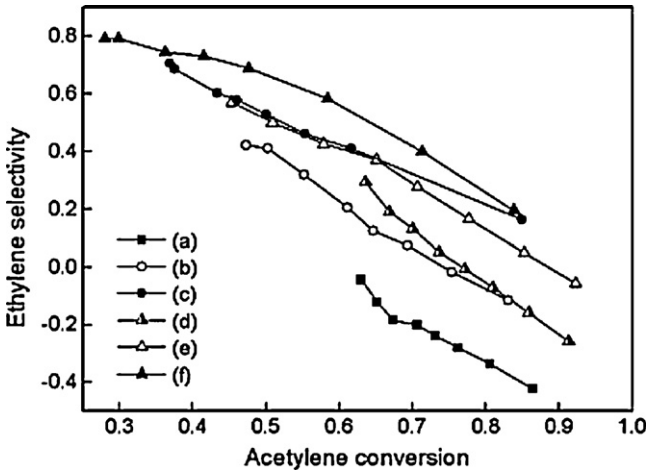

Fig. 26. Changes in ethylene selectivity with the conversion in acetylene hydrogenation for various catalysts: (a) Pd/Al_2O_3; (b) Pd–0.5Ag (I); (c) Pd–1.0Ag (I); (d) Pd–0.2Ag (SR); (e) Pd–0.3Ag (SR); (f) Pd–0.5Ag (SR) [31].

result was obtained because during the SR process Ag was preferentially deposited on the low-coordination sites of Pd, which were responsible for the desorption of highly active sub-surface hydrogen [75–78]. Because the low-coordination sites of Pd were detrimental to ethylene selectivity, Pd–Ag (SR) showed higher ethylene selectivity than Pd–Ag (I). In summary, the higher ethylene selectivity of Pd–Ag (SR) over that of Pd–Ag (I) originated from two aspects of the former catalyst: stronger Pd–Ag interactions due to an intimate contact between two metal components and the preferential decoration of the low-coordination Pd sites by added Ag.

The catalytic performance of Pd–Cu (SR) was affected by added Cu in a manner similar to the case of Pd–Ag (SR) (Fig. 27). Ethylene selectivity was increased, which was also supported by ethylene TPD [32], and the acetylene conversion was decreased by the addition of Cu. The maximum ethylene selectivity of Pd–Cu (SR), which was obtained at a Cu/Pd ratio of 0.41, was comparable to that of a corresponding Pd–0.38 Ag (SR) catalyst. Because the electron density of Pd was modified to smaller extents by Cu than by Ag, as indicated by a smaller shift of the XPS peak for Pd–0.41 Cu (SR) than for Pd–0.38 Ag (SR) (Fig. 28), the strong promotion of ethylene selectivity for Pd–0.41 Cu (SR) was explained by considering an additional factor: the effective decoration of the low-coordination sites of Pd with Cu.

IR observations of CO adsorbed onto the above two types of catalysts (Fig. S5) indicated that the promoter introduced by SR was deposited on the low-coordination sites of Pd, particularly when the promoter amounts were small. When comparing the two promoters, Cu was more selective for deposition on the low-coordination sites than Ag, as indicated by a more significant decrease in the intensity of the linear-CO peak for Pd–Cu (SR) than for Pd–Ag (SR). As the low-coordination Pd sites were detrimental to ethylene selectivity, the decoration of the sites with the promoter resulted in the promotion of ethylene selectivity that was greater with Cu than with Ag. In summary, the weak electronic modification of Pd by Cu was compensated for by the effective decoration of the low-coordination Pd sites with Cu to yield an overall strong promotion of the selectivity.

The reaction results in Fig. 27(b) indicated that a decrease in the activity by promoter addition was much smaller with Pd–Cu (SR) than with Pd–Ag (SR), particularly when the promoter content was smaller than 0.4. As Cu was a weaker electronic modifier of Pd than Ag, it could be expected that the activity was decreased to a smaller extent by the addition of Cu than by the addition of Ag. In addition,

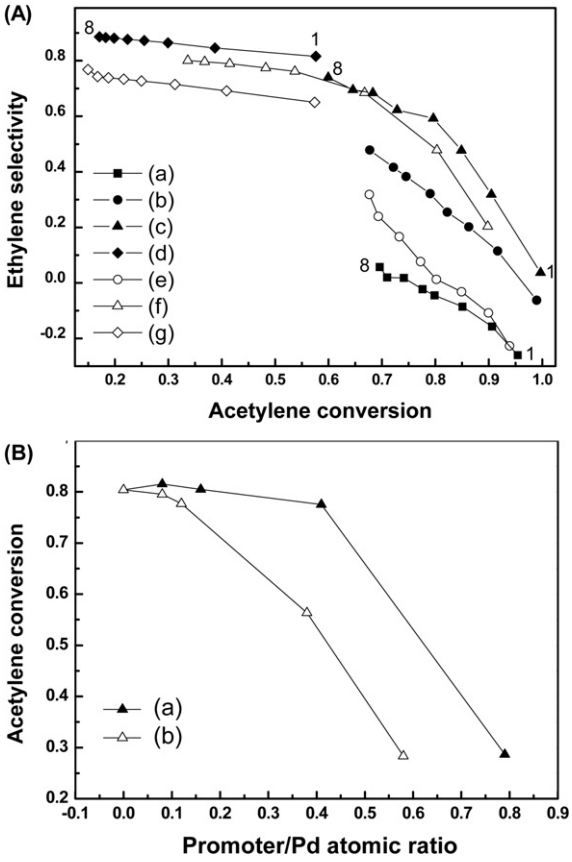

Fig. 27. (A) results of acetylene hydrogenation obtained using Pd/Al_2O_3 containing either Ag or Cu: (a) Pd; (b) Pd–0.08Cu (SR); (c) Pd–0.41Cu (SR); (d) Pd–0.79Cu (SR); (e) Pd–0.08Ag (SR); (f) Pd–0.38Ag (SR); (g) Pd–0.58Ag (SR). (B) Dependence of acetylene conversion on the amount of either Ag or Cu, which was added by the surface redox (SR) method: (a) Pd–*x*Cu (SR); (b) Pd–*x*Ag (SR) [32].

Cu is known to have intrinsic activity for hydrogenation [79–82]. The combination of the above two factors could explain the high activity of Pd–Cu (SR) at a Cu/Pd ratio smaller than 0.4, which was nearly the same as that of un-promoted Pd. Consequently, Pd–0.41 Cu (SR) was developed as an optimum catalyst with the selectivity of Pd–0.38Ag (SR) and the activity of un-promoted Pd.

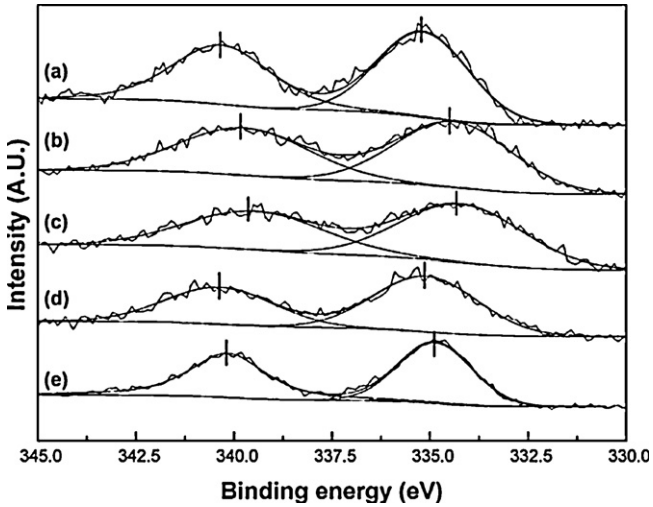

Fig. 28. XPS of Pd obtained from (a) Pd/Al_2O_3; (b) Pd–0.5Ag (I); (c) Pd–0.38Ag (SR); (d) Pd–0.5Cu (I); (e) Pd–0.41Cu (SR) [32].

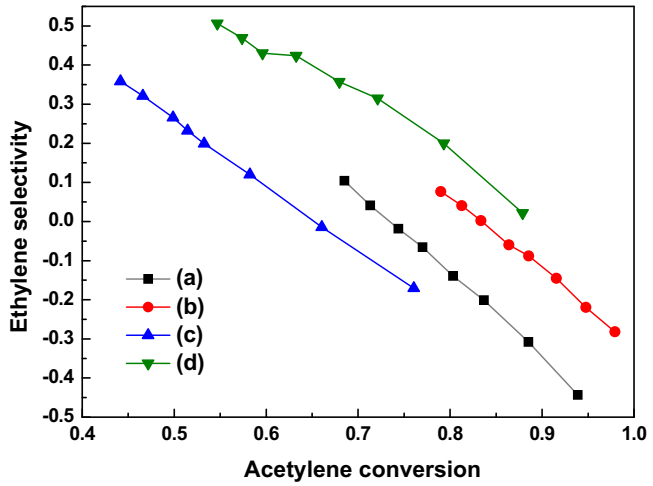

Fig. 29. Reaction results obtained using (a) 1 wt.% Pd/Al_2O_3, (b) 3 wt.% Pd/Al_2O_3 prepared using conventional impregnation (I), and (c) 3 wt.% cubic Pd/Al_2O_3 (Catalyst I), (d) 3 wt.% spherical Pd/Al_2O_3 (Catalyst II) [33].

5.2. Ethylene selectivity of shape-controlled Pd particles

The sensitivity of ethylene selectivity to the surface structure of Pd was further studied using model Pd particles of a uniform size and shape [33]. The particles were prepared from an aqueous solution of Na_2PdCl_4 using polyvinylpyrrolydone (PVP) as a reducing agent and KBr as a capping agent [83]. The particles recovered from the solution had a uniform cubic shape with an average size of 13.6 nm. They were washed with ethanol and hexane, supported on SiO_2, and finally treated sequentially in O_2 and H_2 at 30 °C to remove residual PVP from the surface (Catalyst I). The cubic Pd particles could be transformed to spheres of the same size distribution after treatment in O_2–H_2 cycles at 70 °C (Catalyst II). The IR spectra of CO that was adsorbed onto the catalysts (Fig. S6) indicated that Catalyst II had a peak between 1870 and 1890 cm^{-1}, representing the surface of the Pd(1 1 1) structure, which was in addition to peaks originating from Catalyst I that was in a cubic shape containing the surface of the Pd(1 0 0) structure.

According to the reaction results obtained using the above two catalysts (Fig. 29), Catalyst I was more active than Catalyst II and had a higher ethylene selectivity. The higher activity of Catalyst I, compared with the activity of Catalyst II, originated from the relatively open surface structure of Pd(1 0 0), which allowed easy desorption of sub-surface hydrogen. The results of temperature-programmed hydride decomposition on two catalysts (Fig. 30) indicated that hydride decomposed at temperatures that were lower for Catalyst I than for Catalyst II. Catalyst I had higher ethylene selectivity than Catalyst II because the latter contained a Pd(1 1 1) structure, which lowered the selectivity by allowing ethylene adsorption in the di- and tri-σ bonding modes [84–88].

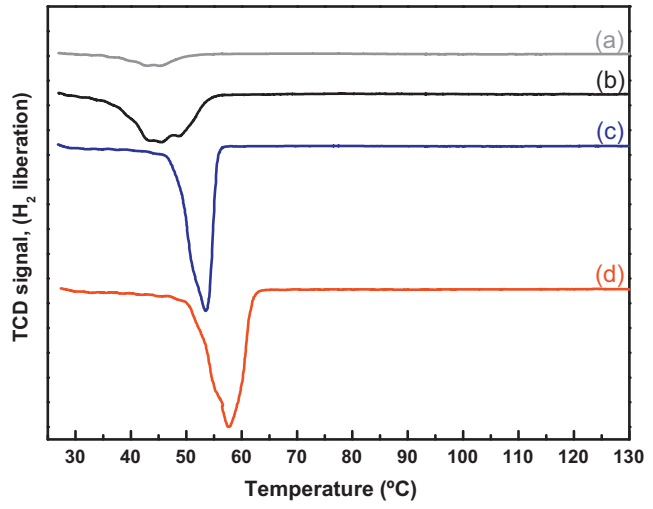

Fig. 30. Temperature-programmed hydride decomposition of (a) 1 wt.% Pd/Al_2O_3, (b) 3 wt.% Pd/Al_2O_3 prepared using conventional impregnation (I), and (c) 3 wt.% cubic Pd/Al_2O_3 (Catalyst I), (d) 3 wt.% spherical Pd/Al_2O_3 (Catalyst II) [33].

6. Conclusions

This article reviewed our previous studies designed to develop good catalysts for use in acetylene hydrogenation based on a few ideas: by adding new promoters, by selectively depositing promoters onto the Pd surface, and by controlling the shape of the Pd particles. Si was selectively deposited on Pd, instead of on the support, by dissociating silane in an H_2 stream. As the Pd surface was decorated with the Si on nearly an atomic scale, the multi-coordination sites of the Pd surface were blocked from the adsorption of ethylene that was produced by acetylene hydrogenation and, as a result, the Si-modified catalysts had higher ethylene selectivity and longer lifetime than those of the un-modified ones. Other promoters studied were oxides of Ti, Nb, and La. We used the oxides as promoters instead of supports. After reduction at 500 °C, the Pd surface was modified with the oxides, which migrated onto the Pd surface. The surface oxides retarded the sintering of the Pd particles and facilitated the desorption of ethylene from the Pd surface, which eventually promoted the ethylene selectivity and extended the lifetime of the catalysts. The extent of promotion was different depending on the added oxide. Promoters extended the catalyst lifetime by modifying the Pd surface either electronically or geometrically, such that the desorption of 1,3-butadiene, a precursor of green oil, was facilitated, and the polymerization of 1,3-butadiene on the Pd surface was suppressed. The ethylene selectivity of Pd was promoted with Cu or Ag to a greater extent when the promoter was added by a surface redox method instead of a conventional impregnation method because the former method allowed the preferential deposition of the promoter onto the edge sites of Pd, which are known to lower ethylene selectivity. The structure sensitivity of the catalyst was further studied using nanoscale Pd particles of a uniform size but of different shapes, i.e., cubes and spheres, which had different surface crystal structures. Reaction results indicated that ethylene selectivity was higher on cubes than on spheres, suggesting the possibility of designing new catalysts based on the control of their surface structures.

Acknowledgements

This work was supported by the Human Resources Development of the Korea Institute of Energy Technology Evaluation Planning (KETEP) grant funded by the Korea Government Ministry of Knowledge Economy (No. 20104010100510) and Basic Science Research Program through the National Research Foundation of Korea (NRF) funded by the Ministry of Education, Science and Technology (2011-0005392) (for W.-J.K.); by BASF Aktiengesellschaft, the Brain Korea 21 project, and the Korea Science and Engineering Foundation (KOSEF) through the National Research Laboratory Program (for S.H.M.).

Appendix A. Supplementary data

Supplementary data associated with this article can be found, in the online version, at doi:10.1016/j.cattod.2011.09.037.

References

[1] W.K. Lam, L. Lloyd, Oil Gas J. 27 (1972) 66–70.
[2] G.C. Bond, Catalysis by Metals, Academic Press, New York, 1962, pp. 281–309.
[3] G. Ertl, H. Knözinger, J. Weitkamp, Handbook of Heterogeneous Catalysts, vol. 5, VCH, Weinheim, Germany, 1997, pp. 2165–2186.
[4] A. Molnar, A. Sarkany, M. Varga, J. Mol. Catal. A: Chem. 173 (2001) 185–221.
[5] D.L. Trimm, Design of Industrial Catalysts, Elsevier, Amsterdam, 1980, pp. 229–232.
[6] D.C. Huang, K.H. Chang, W.F. Pong, P.K. Tseng, K.J. Hung, W.F. Hung, Catal. Lett. 53 (1998) 155–159.
[7] P. Miegge, J.L. Rousset, B. Tardy, J. Massardier, J.C. Bertolini, J. Catal. 149 (1994) 404–413.
[8] S. Leviness, V. Nair, A.H. Weiss, J. Mol. Catal. 25 (1984) 131–140.
[9] V.H. Sandoval, C.E. Gigola, Appl. Catal. A 148 (1996) 81–96.
[10] L. Cerveny, I. Paseka, K. Surma, N.T. Thanh, V. Ruzicka, Collect. Czech. Chem. Commun. 5 (1985) 61–70.
[11] J.P. Boitiaux, J. Cosyns, M. Derrien, G. Leger, Hydrocarbon Process. (1985) 51–59.
[12] Y.H. Park, G.L. Price, Ind. Eng. Chem. Res. 31 (1992) 469–474.
[13] E.W. Shin, C.H. Choi, K.S. Chang, Y.H. Na, S.H. Moon, Catal. Today 44 (1998) 137–143.
[14] J.H. Kang, E.W. Shin, W.J. Kim, J.D. Park, S.H. Moon, J. Catal. 208 (2002) 310–320.
[15] Y.H. Park, G.L. Price, Ind. Eng. Chem. Res. 30 (1991) 1693–1699.
[16] D. Duca, F. Frusteri, A. Parmaliana, G. Deganello, Appl. Catal. A 146 (1996) 269–284.
[17] M.L. Derrien, Stud. Surf. Sci. Catal. 27 (1986) 613–666.
[18] J. Margitfalvi, L. Guczi, A.H. Weiss, J. Catal. 72 (1981) 185–198.
[19] J.M. Moses, A.H. Weiss, K. Matusek, L. Guczi, J. Catal. 86 (1984) 417–426.
[20] A. Sarkany, A.H. Weiss, L. Guczi, J. Catal. 98 (1986) 550–553.
[21] A.L. Backman, R.I. Masel, J. Vac. Sci. Technol. A9 (1991) 1789–1792.
[22] T.P. Beebe Jr., M.R. Albert, J.T. Yates Jr., J. Am. Chem. Soc. 108 (1986) 663–671.
[23] M. Larsson, J. Jansson, S. Asplund, J. Catal. 178 (1998) 49–57.
[24] G.C. Battiston, L. Dalloro, G.R. Tauszik, Appl. Catal. 2 (1982) 1–17.
[25] E.W. Shin, J.H. Kang, W.J. Kim, J.D. Park, S.H. Moon, Appl. Catal. A 223 (2002) 161–172.
[26] J.H. Kang, E.W. Shin, W.J. Kim, J.D. Park, S.H. Moon, Catal. Today 63 (2000) 183–188.
[27] W.J. Kim, E.W. Shin, J.H. Kang, S.H. Moon, Appl. Catal. A 251 (2003) 305–313.
[28] W.J. Kim, J.H. Kang, I.Y. Ahn, S.H. Moon, Appl. Catal. A 268 (2004) 77–82.
[29] W.J. Kim, J.H. Kang, I.Y. Ahn, S.H. Moon, J. Catal. 226 (2004) 226–229.
[30] I.Y. Ahn, W.J. Kim, S.H. Moon, Appl. Catal. A 308 (2006) 75–81.
[31] J.H. Lee, S.K. Kim, I.Y. Ahn, W.-J. Kim, S.H. Moon, Catal. Commun. 12 (2011) 1251–1254.
[32] S.K. Kim, J.H. Lee, I.Y. Ahn, W.-J. Kim, S.H. Moon, Appl. Catal. A 401 (2011) 12–19.
[33] S.K. Kim, C. Kim, J.H.J. Kim, H. Lee, S.H. Moon, The 13th Korea–Japan Symposium on Catalysis, Jeju, May 23–25, 2011, p. 072.
[34] A. Sarkany, A.H. Weiss, L. Guczi, Appl. Catal. 10 (1984) 369–388.
[35] D. Tessier, A. Rakai, B. Verduraz, J. Chem. Soc. Faraday Trans. 88 (1992) 741–749.
[36] G.V. Smith, S. Tjandra, M. Musoiu, T. Wiltowski, F. Notheisz, M. Bartok, I. Hannus, D. Ostgard, V. Malhotra, J. Catal. 161 (1996) 441–450.
[37] G.V. Smith, J. Stoch, S. Tjandra, T. Wiltowski, Catalysis of Organic Reactions, Marcel Decker, New York, 1995, p. 403.
[38] J.A. Konvalinka, J.J.F. Scholten, J. Catal. 48 (1977) 374–385.
[39] A. Rochefort, J. Andzelm, N. Russo, D.R. Salahub, J. Am. Chem. Soc. 112 (1990) 8229.
[40] E.M. Stuve, R.J. Madix, J. Phys. Chem. 89 (1985) 105–112.
[41] G.A. Somorjai, D.W. Blakelv, Nature 258 (1975) 580–583.
[42] A.J. Den Hartog, M. Deng, F. Jongerius, V. Ponec, J. Mol. Catal. 60 (1990) 99.
[43] S.J. Tauster, S.C. Fung, J. Catal. 55 (1978) 29–35.
[44] S.J. Tauster, S.C. Fung, R.L. Garten, J. Am. Chem. Soc. 100 (1978) 170–175.
[45] J. Santos, J. Phillips, J.A. Dumesic, J. Catal. 81 (1983) 147–167.
[46] H.R. Sadeghi, V.E. Henrich, J. Catal. 87 (1984) 279–282.
[47] A.J. Simoens, R.T.K. Baker, D.J. Dwyer, C.R.F. Lund, R.J.J. Madon, J. Catal. 86 (1984) 359–372.
[48] Y.-W. Chung, G. Xiong, C.C. Kao, J. Catal. 85 (1984) 237–243.
[49] C.S. Ko, R.J.J. Gorte, J. Catal. 90 (1984) 59–64.
[50] G.B. Raupp, J.A. Dumesic, J. Catal. 95 (1985) 587–601.
[51] J.M. Herrmann, M. Gravelle-Rumeau-Maillot, P.C. Gravelle, J. Catal. 104 (1987) 136.
[52] P. Chou, M.A. Vannice, J. Catal. 104 (1987) 1–16.
[53] M.K. Bahl, S.C. Tsai, Y.W. Chung, Phys. Rev. B 21 (1980) 1344–1348.
[54] S.C. Fung, J. Catal. 76 (1982) 225–230.
[55] C.C. Kao, S.C. Tsai, M.K. Bahl, Y.W. Chung, W.J. Lo, Surf. Sci. 95 (1980) 1–14.
[56] Y. Lee, Y. Inoue, I. Yasumori, Bull. Chem. Soc. Jpn. 54 (1981) 3711–3716.
[57] D. Briggs, J. Dewing, A.G. Burden, R.B. Moyes, P.B. Wells, J. Catal. 65 (1980) 31–35.
[58] D. Duca, F. Frusteri, A. Parmaliana, G. Deganello, Appl. Catal. A 146 (1996) 269–285.
[59] T.H. Fleisch, R.F. Hicks, A.T. Bell, J. Catal. 87 (1984) 398–413.
[60] N.S. Figoli, P.C. L'Argentiere, A. Arcoya, X.L. Seoane, J. Catal. 155 (1995) 95–105.
[61] X.L. Seoane, N.S. Figoli, P.C. L'Argentiere, J.A. Gonzalez, A. Arcoya, Catal. Lett. 47 (1997) 213–220.
[62] C. Yang, J. Ren, Y. Sun, Catal. Lett. 84 (2002) 123–129.
[63] R.B. Moyes, P.B. Wells, J. Grant, N.Y. Salman, Appl. Catal. 229 (2002) 251–259.
[64] A. Borgschulte, J.H. Rector, B. Dam, R. Griessen, A. Zuttel, J. Catal. 235 (2005) 353–358.
[65] A. Borgschulte, W. Lohstroh, R.J. Westerwaal, H. Schreuders, J.H. Rector, B. Dam, R. Griessen, J. Alloys Compd. 404–406 (2005) 699–705.
[66] M.S. Spencer, J. Phys. Chem. 88 (1984) 1046–1047.
[67] S. Asplund, J. Catal. 158 (1996) 267–278.
[68] M. Larsson, J. Jansson, S. Asplund, J. Catal. 162 (1996) 365–367.
[69] I.Y. Ahn, J.H. Lee, S.S. Kum, S.H. Moon, Catal. Today 123 (2007) 151–157.
[70] W.J. Kim, C.H. Choi, S.H. Moon, Korean J. Chem. Eng. 19 (4) (2002) 617–621.
[71] A.H. Weiss, S. Leviness, V. Nair, L. Guczi, A. Sarkany, Z. Schay, Proceedings of the 8th International Congress on Catalysis, vol. 5, 1984, pp. 591–599.
[72] I.Y. Ahn, J.H. Lee, S.K. Kim, S.H. Moon, Appl. Catal. A 360 (2009) 38–42.
[73] S.J. Thomson, G. Webb, J. Chem. Soc. Chem. Commun. 13 (1976) 526–527.
[74] A. Borodzinski, G.C. Bond, Catal. Rev. 48 (2006) 91–144.
[75] H. Okuyama, W. Siga, N. Takagi, M. Nishijima, T. Aruga, Surf. Sci. 401 (1998) 344–363.
[76] S.T. Ceyer, Acc. Chem. Res. 34 (2001) 737–744.
[77] A.M. Doyle, S.K. Shaikhutdinov, S.D. Jackson, H.-J. Freund, Angew. Chem. Int. Ed. 42 (2003) 5240–5243.
[78] M. Morkel, G. Rupprechter, H.-J. Freund, Surf. Sci. 588 (2005) L209–L219.
[79] J.T. Wehrli, D.J. Thomas, M.S. Wainwright, D.L. Trimm, N.W. Cant, Appl. Catal. 66 (1990) 199–208.
[80] J.T. Wehrli, D.J. Thomas, M.S. Wainwright, D.L. Trimm, N.W. Cant, Appl. Catal. 70 (1991) 253–262.
[81] J.T. Wehrli, D.J. Thomas, M.S. Wainwright, D.L. Trimm, N.W. Cant, Stud. Surf. Sci. Catal. 75 (1993) 2289–2292.
[82] F. Studt, F. Abild-Pedersen, T. Bligaard, R.Z. Sørensen, C.H. Christensen, J.K. Nørskov, Angew. Chem. Int. Ed. 47 (2008) 9299–9302.
[83] B. Lim, et al., Adv. Funct. Mater. 19 (2009) 189–200.
[84] J. Margitfalvi, L. Guczi, A.H. Weiss, React. Kinet. Catal. Lett. 15 (1981) 475–479.
[85] E.H. Van Broekhoven, J.W.F.M. Schoonhoven, V. Ponec, Surf. Sci. 156 (1985) 899–910.
[86] E.H. Van Broekhoven, V. Ponec, J. Mol. Catal. 25 (1984) 109–118.
[87] C. Kemball, Catal. Rev.: Sci. Eng. 5 (1972) 33–53.
[88] A.J.D. Hartog, M. Deng, F. Jongerius, V. Ponec, J. Mol. Catal. 60 (1990) 99–108.